

REMARKS

Applicants respectfully request reconsideration of the present application in view of the foregoing amendments and in view of the reasons that follow.

I. Summary of the Claims

Claim 46 is currently being amended.

This amendment adds, changes and/or deletes claims in this application. A detailed listing of all claims that are, or were, in the application, irrespective of whether the claim(s) remain under examination in the application, is presented, with an appropriate defined status identifier.

After amending the claims as set forth above, claims 45-52 are now pending in this application.

II. Rejection Under 35 U.S.C. § 103(a)

The Examiner rejected claims 45-52 under 35 U.S.C. § 103(a) for allegedly being unpatentable over International Publication No. WO 02/16418 to Alnemri ("Alnemri") in view of International Publication No. WO 02/16402 to Wang ("Wang") and Ford *et al.*, *Gene Therapy* 8:1-4 (2001) ("Ford"). Office Action at 2. Applicants respectfully traverse this ground for rejection.

1. The Ford Reference Teaches Away From the Claimed Invention

The Examiner concurs with Applicants' point that Ford "discloses that the full-length TAT protein stimulates growth of Kaposi's sarcoma derived cells and that TAT transgenic mice develop Kaposi sarcoma...." Office Action at 3. However, the Examiner maintains that Ford "expressly teaches that PTD [protein transduction domain] may provide efficient means of intracellular delivery of not just proteins, but macromolecules such as DNA as well as cancer chemotherapeutic agents (e.g. doxorubicin)...[and] for efficient antigen loading of dendritic cells for a range of vaccination purposes, including anti-tumor immune therapy...." *Id.* (emphasis in original) (text in brackets added).

The Examiner's arguments fail to recognize that Ford teaches away from the specific use of the TAT protein for delivery of proteins for the treatment of cancer. Specifically, one of skill in the art would not have considered using the TAT protein to deliver a protein to induce apoptosis in tumor cells due to its ability to transactivate genes and induce proliferation of cancer cells, thus negating any potential apoptotic-inducing effects of the cancer therapy. Indeed Ford states that "if the 11 aa TAT PTD (amino acids 47-57) is shown to be devoid of toxic effects *in vivo*, it will be of tremendous use in a variety of potential applications." Ford at 2-3 (emphasis added).

The Examiner points to the use of PTDs for delivering cancer therapeutic agents such as methotrexate and doxorubicin as described in Ford. Office Action at 3. Ford cites two papers by Hamstra *et al.*, *Cancer Res.* 60:657-665 (2000) (Hamstra) (filed herewith as Exhibit A) and Rouselle *et al.*, *Pharma and Exper. Therapeutics*, 57:679-686 (2000) (Rouselle) (filed herewith as Exhibit B), to support the use of PTDs for delivering methotrexate and doxorubicin. Neither paper describes the use of the TAT protein linked to a chemotherapeutic agent. Indeed Rouselle describes the coupling of doxorubicin to D-penetratin (derived from Antennapedia) and SynB1. *See* Rouselle at Abstract and 680. The Hamstra paper describes a methotrexate- α -peptide prodrug and does not describe attachment of MTX to any of the PTDs described in Ford. *See* Hamstra at Abstract. Furthermore, the Examiner's reference to the anti-tumor immune therapy in Ford is misplaced in this context as the antigen loading of dendritic cells is quite different from inducing apoptosis.

The Examiner maintains that "one skilled in the art would have been motivated to use TAT PTD to deliver the Smac protein in view of Fold [*sic*] because Fold [*sic*] disclose [*sic*] that many proteins including small peptides have been successfully transported into a wide variety of human and murine cell types using the TAT PTD methodology." Office Action at 3. However, this reasoning fails to take into consideration that one of skill in the art attempting to solve the problem of delivering a protein for use in treating cancer by the induction of apoptosis would not have been motivated to attach the agent to a protein which has been shown to have a contrary effect, *i.e.* induces the growth of tumor cells. The Examiner assumes that one of ordinary skill is merely attempting to solve the problem of

delivering a protein into a cell without taking into account that the protein is being delivered into the cell to develop an improved cancer therapy. Thus, one of skill in the art would not have been motivated to modify the Smac peptides of Alnemri or Wang by attaching the TAT peptide of Ford for delivery of a protein as part of an anti-cancer therapy.

2. The Examiner is Relying Upon Impermissible Hindsight

In the present rejection, the Examiner relies upon impermissible hindsight to selectively pick individual elements of the claimed invention from the cited references to assert an alleged case of *prima facie* obviousness. It is well established that "[o]ne cannot use hindsight reconstruction to pick and chose among isolated disclosures in the prior art to deprecate the claimed invention." *In re Fine*, 5 USPQ2d 1596, 1600 (Fed. Cir. 1988); *see also* MPEP § 2141(II)(c). This point was also emphasized by the Supreme Court in *KSR Int'l Co. v. Teleflex, Inc.* 127 S.Ct. 1727 (2007). "A factfinder should be aware, of course, of the distortion caused by hindsight bias and must be cautious of arguments reliant upon *ex post* reasoning." *KSR* at 1742.

Claims 45-52 relate to a Smac carrier or a composition comprising the Smac carrier comprising a Smac protein comprising amino acids 56 to 59; 56 to 62; or 56 to 70 of the Smac protein of SEQ ID NO:1. Of the proteins disclosed in Alnemri and Wang, the Examiner has not provided a reason or motivation why one of skill in the art would have chosen these particular sequences.

Furthermore, the Examiner has failed to show any reason or motivation for one of skill in the art to have selected TAT, or fragments of TAT, over the other disclosed transducing polypeptides of Ford such as Antennapedia or the herpes simplex virus VP22 protein to link to the claimed Smac fragments, as discussed above. Indeed, the Examiner stated that "[w]hether one skilled in the art would have also been motivated to use Antennapedia or herpes simplex virus VP22 protein as a carrier protein for Smac is irrelevant to this rejection." Office Action at 3. However, Applicants respectfully disagree. The Examiner is required to consider the reference as a whole, especially to avoid impermissible hindsight reasoning. *W.L. Gore & Associates, Inc. v. Garlock, Inc.*, 721 F.2d 1540 (Fed. Cir.

1983) (A prior art reference must be considered in its entirety, *i.e.*, as a whole, including portions that would lead away from the claimed invention.). Based on the disclosure in Ford regarding the TAT protein described above, one of skill in the art would have been motivated to use the PTD of Antennapedia or VP22 and not the PTD of TAT.

The Examiner has used the claimed invention itself as a roadmap to allege that the claims are obvious over the cited combination of references. To suggest now that it would be obvious to chose the claimed Smac protein fragments linked to the TAT protein or fragments thereof, based on the disclosures of Alnemri, Wang and Ford, can only be a result of hindsight.

3. No Reasonable Expectation of Success

Applicants argue that one of skill in the art would have had no reasonable expectation of success in modifying the Smac peptides of Alnemri and Wang with the TAT protein of Ford to arrive at a peptide which was able, in combination with other anti-cancer agents, to treat cancer *in vivo*. "A rationale to support a conclusion that a claim would have been obvious is that all the claimed elements were known in the prior art and one skilled in the art could have combined the elements as claimed by known methods *with no change in their respective functions, and the combination would have yielded nothing more than predictable results to one of ordinary skill in the art.*" MPEP § 2143.02 citing *KSR*, 127 S. Ct. at 1731 (emphasis added).

The experiments with Smac peptides, as described by Alnemri and Wang, which were actually performed were limited to experiments *in vitro*. See Alnemri at Examples 2-5 and Wang at Examples 9-16¹. The Examiner has previously stated that both Alnemri and Wang teach Smac peptides for "inducing cell cancer apoptosis". See Office Action dated October 1, 2007 at 24 and 25. However, one of skill in the art would have had no reasonable expectation of success that the Smac peptides presently claimed would induce apoptosis of cancer cell *in*

¹ Examples 17, 18 and 19 of Wang describe *in vivo* assays for testing AV peptoids as anti-cancer agents, however the Examples are written in the future or mixed tense indicating that they are prophetic examples. Additionally, Example 19 comments on the efficacy of "peptoids" in the WAP-RAS Transgenic model, however it is not clear if the experiments were actually performed, if Smac peptides were used, and what the actual results were since no data is presented.

vivo. In fact, as is shown in the Examples of the present application, Smac peptides alone did not result in an anti-tumor effect *in vivo*. Rather the Smac peptides enhanced the anti-tumor effect of another polypeptide, TRAIL. See specification at ¶[0058] ("Importantly, Smac peptides significantly sensitized glioblastoma cells for TRAIL-induced apoptosis, while treatment with Smac peptides alone showed no anti-tumor effect.") and Fulda *et al.*, *Nature Medicine* 8:808-815 (2002) (submitted as document A21 with the IDS filed January 19, 2005).

The Examiner has stated that the treatment of cancer is unpredictable: "the fundamental problem in drug discovery for cancer is that the model systems are not predictive." *Id.* at 19. Moreover, "[e]ven if a candidate drug inhibits cancer cell proliferation *in vitro*, it is still unpredictable where this drug will be effective in treating cancer *in vivo*, such as in an animal model." *Id.* at 19. Therefore, it is not reasonable to draw conclusions from the *in vitro* experiments described in Alnemri and Wang.

Applicants have shown that the claimed fusion peptides in a glioblastoma tumor model significantly sensitized glioblastoma cells for apoptosis. The use of the claimed peptides alone did not show an anti-tumor effect. Thus, there was no reasonable expectation of success in creating a cancer therapy which would be effective *in vivo* based on the cited art (*i.e.* the Smac peptides of Alnemri and Wang fused to the TAT-peptide of Ford).

Thus, the Examiner has failed to make a *prima facie* case of obviousness as: 1) the Ford reference teaches away from the claimed invention; 2) the Examiner relies upon impermissible hindsight reasoning; and 3) there was no reasonable expectation of success for one of skill in the art to arrive at the claimed invention based on the cited art. As such, Applicants respectfully request that the Examiner reconsider and withdraw the rejection.

III. Objections to the Claims

The Examiner objected to claim 46 because the claim recited "amino acid sequence 47 to 47 SEQ ID NO:3." Office Action at 4. Per the Examiner's suggestion, Applicants have amended claim 46 to include the word "of" just prior to the term "SEQ ID NO:3." Thus, Applicants believe this objection to be moot.

IV. Notice to Comply With Sequence Rules

The Examiner alleges that the application fails to comply with the requirements of 37 C.F.R. 1.821 through 1.825 as Applicants allegedly failed to provide a statement that the content of the paper and computer readable copies are the same, and where applicable, include no new matter. Office Action at 5.

Applicants respectfully assert that the statement under 37 C.F.R. § 1.821(f) that the content of the paper and computer readable copy of the sequence listing is the same is not necessary in the present application. Applicants filed the sequence listing electronically via EFS-Web on April 1, 2008. By filing on EFS-Web the paper copy and the computer readable copy of the sequence listing are one in the same and therefore a statement pursuant 37 C.F.R. § 1.821(f) is not required. Indeed on the USPTO web site under EFS-web Help, FAQ's, p200efs152 entitled "Is a statement required verifying that the computer readable format (CRF) and paper copy of a sequence listing are the same?" states:

If a sequence listing text file submitted via EFS-Web complies with the requirements of 37 CFR 1.824, the filer need not submit i) any additional copies of the sequence listing pursuant to 37 CFR 1.821(e) **nor ii) the statement described in 37 CFR 1.821(f).**

Additionally, Applicants point the Examiner's attention to the Amendment and Reply filed April 1, 2008 in which Applicants stated that "the amendment to include the sequence listing filed herewith does not introduce new matter" pursuant to 37 C.F.R. § 1.825. Reply at 10.

Thus, Applicants believe the present application to be in compliance with all sequence rules and respectfully request the Examiner to acknowledge compliance.

V. Conclusion

Applicants believe that the present application is now in condition for allowance. Favorable reconsideration of the application as amended is respectfully requested.

The Examiner is invited to contact the undersigned by telephone if it is felt that a telephone interview would advance the prosecution of the present application.

The Commissioner is hereby authorized to charge any additional fees which may be required regarding this application under 37 C.F.R. §§ 1.16-1.17, or credit any overpayment, to Deposit Account No. 19-0741. Should no proper payment be enclosed herewith, as by a check being in the wrong amount, unsigned, post-dated, otherwise improper or informal or even entirely missing or a credit card payment form being unsigned, providing incorrect information resulting in a rejected credit card transaction, or even entirely missing, the Commissioner is authorized to charge the unpaid amount to Deposit Account No. 19-0741. If any extensions of time are needed for timely acceptance of papers submitted herewith, Applicant hereby petitions for such extension under 37 C.F.R. §1.136 and authorizes payment of any such extensions fees to Deposit Account No. 19-0741.

Respectfully submitted,

Date February 18, 2009

FOLEY & LARDNER LLP
Customer Number: 22428
Telephone: (202) 672-5538
Facsimile: (202) 672-5399

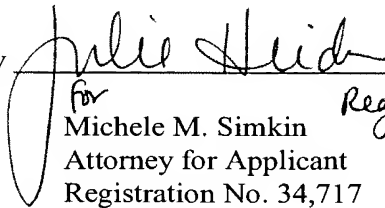
By 
for Michele M. Simkin Reg # 54,161
Attorney for Applicant
Registration No. 34,717

EXHIBIT A

Expression of Endogenously Activated Secreted or Cell Surface Carboxypeptidase A Sensitizes Tumor Cells to Methotrexate- α -Peptide Prodrugs¹

Daniel A. Hamstra, Michel Pagé, Jonathan Maybaum, and Alnawaz Rehemtulla²

Departments of Pharmacology [D. A. H., J. M.] and Radiation Oncology [D. A. H., J. M., A. R.], The University of Michigan, Ann Arbor, Michigan 48109-0582, and Department of Biochemistry, The University of Laval, Laval, Quebec, Canada G1K 7P4 [M. P.]

ABSTRACT

Methotrexate (MTX) is one of the most commonly used agents in the treatment of solid malignancies; however, the toxicities of MTX to bone marrow and gastrointestinal tract complicate this therapy. We, therefore, propose a gene-dependent enzyme prodrug therapy to limit these toxicities by localizing the production of MTX to the site of the tumor. The combination of MTX- α -peptide prodrugs, which cannot be internalized by the cellular reduced folate carrier, with carboxypeptidase A (CPA), which can remove the blocking peptide, has been demonstrated previously *in vitro* using antibody-dependent enzyme prodrug therapy. CPA is normally synthesized as a zymogen that is inactive without proteolytic removal of its propeptide by trypsin. Therefore, to adapt this system to gene-dependent enzyme prodrug therapy, a mutant form of CPA was engineered, CPA_{ST3}, that does not require trypsin-dependent zymogen cleavage but is instead activated by ubiquitously expressed intracellular propeptidases. Purification, peptide sequencing, and kinetic analysis indicated that mature CPA_{ST3} is structurally and functionally similar to the trypsin-activated, wild-type enzyme. In addition, CPA_{ST3}-expressing tumor cells were sensitized to MTX prodrugs in a dose- and time-dependent manner. To limit diffusion of CPA, a cell surface localized form was generated by constructing a fusion protein between CPA_{ST3} and the phosphatidylinositol linkage domain from decay accelerating factor. SDS-PAGE and flow cytometric analysis of infected tumor cells indicated that CPA_{DAF} was cell surface localized. Finally, after retroviral transduction, this enzyme/prodrug strategy exhibited a potent bystander effect, even when <10% of the cells were transduced, because extracellular production of MTX sensitized both transduced and nontransduced cells.

INTRODUCTION

Chemotherapeutics, drugs that are preferentially toxic to tumor cells as compared with host tissues, are a vital part of most current cancer treatments. However, most common chemotherapeutic agents have a small therapeutic index and exhibit profound systemic toxicities, particularly to rapidly dividing tissues such as bone marrow and gastrointestinal tract (1). These toxicities present a significant morbidity and mortality; in addition, they limit the dose of chemotherapeutic used and thus may also decrease the clinical response. One method proposed to circumvent these toxicities and to increase the therapeutic index of chemotherapy is the development of GDEPT³ (reviewed in Ref. 2): (a) tumors are transduced with the gene for an

enzyme whose activity is not normally present in the host; and (b) a prodrug is administered systemically, which is nontoxic except when metabolically converted to a toxic form by the enzyme transduced in the first step. The goal of these strategies is to simultaneously increase the local concentration of the toxic agent while also decreasing the associated systemic toxicities.

MTX, a folate analogue antimetabolite, is one of the most commonly used chemotherapeutics for the treatment of solid malignancies (3, 4). Prodrugs of MTX have been described where a blocking amino acid is conjugated to the glutamic acid residue in MTX; these prodrugs are unable to be internalized by the cellular reduced folate carrier (5). CPA, a zinc-metalloprotease, is normally synthesized in the pancreas and released into the lumen of the small intestine, where trypsin-dependent zymogen activation is necessary to remove the inhibitory propeptide and activate the enzyme (6). CPA has been described previously for use in ADEPT protocols in conjunction with MTX- α -peptide prodrugs (5, 7, 8). All of these ADEPT strategies relied upon purified CPA that was activated by trypsin *in vitro* to remove the propeptide. However, ADEPT systems are plagued by a number of problems, including cost and difficulties with development and purification of antibodies, immunogenicity of antibodies, accessibility of tumor to the enzyme/antibody conjugate, stability of the enzyme/antibody conjugate, and background conversion of prodrugs because of localization of antibody conjugates to inappropriate tissues (2). To adapt this CPA/MTX- α -peptide-based strategy from an antibody-based therapy to a GDEPT, we endeavored to generate mutant forms of CPA that would be activated in a trypsin-independent manner by endogenous cellular proteases.

PACE/furin is the prototypical member of a family of PCs that include at least seven members (9). These serine proteases are involved in the maturation of secretory proteins by cleavage after clusters of basic amino acids in proteins such as: growth factors, growth factor receptors, prohormones, bacterial toxins, and viral coat proteins. Some of the PCs exhibit restrictive expression in neuroendocrine tissues; however, at least three members of the family, PACE, PACE4, and PC7, appear to be ubiquitously expressed (9). Therefore, we felt that a mutant form of CPA, which was engineered to be activated by one or more of these PCs, could prove to be an effective part of a GDEPT strategy. Previously, we have reported just such a mutant, CPA₉₅, where a simple tetra-basic PACE cleavage site (-RQKR-) was introduced into CPA between the propeptide and the mature enzyme (10). CPA₉₅ was expressed as an active enzyme independent of trypsin treatment and could sensitize cells to MTX-Phe. This activation, however, was dependent upon overexpression of PACE with little or no activation detected by endogenous PCs in absence of PACE cotransfection. To overcome the need for exogenous PACE expression, we report here a mutant form of CPA (CPA_{ST3}) that is fully activated in a trypsin-independent manner by endogenous propeptidases. The rationale for the construction of CPA_{ST3} was that the 10 amino acid sequence (-GLSARNRQKR-) within ST3 sensitizes it to activation by PACE (11). Because this sequence encompasses the key features of a PACE cleavage site (*i.e.*, basic residues at -1, -2, -4, and -6 relative to cleavage; Ref. 12), we

Received 3/31/99; accepted 12/2/99.

The costs of publication of this article were defrayed in part by the payment of page charges. This article must therefore be hereby marked *advertisement* in accordance with 18 U.S.C. Section 1734 solely to indicate this fact.

¹Supported in part by NIH Award IR29CA7390401 (to A. R.), USAMRC Breast Cancer Research Pre-Doctoral Fellowship DAMD17-97-1-7127 (to D. H.), as well as a Developmental Student Award (to D. H.) as part of the UM Specialized Programs of Research Excellence in Prostate Cancer P50 CA69568. D. H. is a fellow in the Medical Scientist Training Program.

²To whom requests for reprints should be addressed, at The University of Michigan Medical School, 1331 East Ann Street, Ann Arbor, MI 48105-0582. Phone: (734) 764-4209; Fax: (734) 763-1581; E-mail: alnawaz@umich.edu.

³The abbreviations used are: GDEPT, gene-dependent enzyme/prodrug therapy; MTX, methotrexate; MTX-Phe, methotrexate- α -phenylalanine; CPA, carboxypeptidase A1; ADEPT, antibody-dependent enzyme/prodrug therapy; PACE, paired basic amino acid cleaving enzyme; PC, prohormone convertase; HPLC, high-performance liquid chromatography; HSV-TK, herpes simplex virus thymidine kinase; CFA, colony formation assay; SF, surviving fraction; IRES, internal ribosomal entry site; ST3, stromelysin 3; DAF, decay accelerating factor; 5-FC, 5-fluorocytosine; HD, high dose.

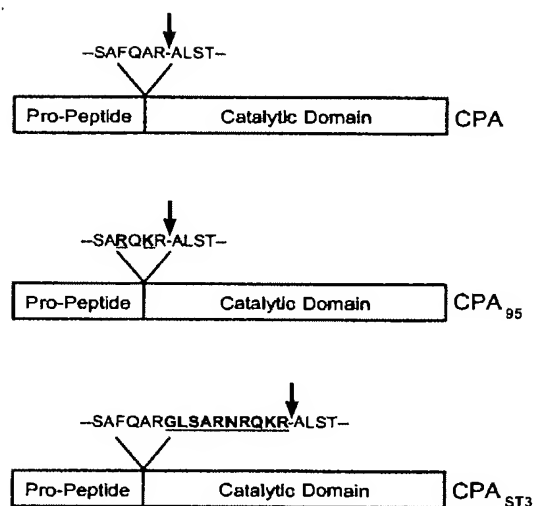


Fig. 1. Mutations introduced into the CPA protein to facilitate subtilisin-like propeptidase cleavage. Wild-type CPA, CPA₉₅, and CPA_{ST3} are depicted in diagrammatic form, mutated residues are underlined, and the cleavage sites are indicated with an arrow.

hypothesized that the insertion of this decapeptide would also sensitize CPA_{ST3} to PC-based activation.

The secretion of active CPA into the extracellular space should allow for a potent bystander effect where a small population of CPA expressing cells could generate sufficient MTX within the tumor milieu to sensitize adjacent, nontransduced cells. This is particularly true for this enzyme/prodrug system because the MTX is generated outside the transduced cell, so both CPA-expressing and bystander cells should be equally sensitized. Unfortunately, if active secreted CPA is able to diffuse out of the tumor, it might result in both a decreased local production and in increased systemic generation of MTX. Therefore, to restrict CPA to the site of transduction, we constructed a cell surface tethered form of the enzyme by fusing CPA_{ST3} to the glycopospholipid membrane linkage domain of DAF (13). This fusion protein is anchored to the surface of the cell by a lipid linkage and thus may afford local production of MTX without systemic release of the protein. In this report, the generation of both the endogenously active soluble and cell surface forms of CPA are described, as is their ability to use MTX- α -peptide prodrugs and sensitize cells *in vitro*.

MATERIALS AND METHODS

Expression Plasmids. All common molecular biological techniques were performed according to Sambrook *et al.* (14). The expression plasmids for wild-type rat CPA, the single PACE cleavage mutant of CPA at amino acid 95 (CPA₉₅), PACE, or the dominant-negative form of PACE (PACE.SA) have all been described previously (10, 12). The endogenously activated mutant of CPA (CPA_{ST3}) and the cell surface-localized form of this mutant (CPA_{DAF}) were constructed by overlap PCR (15) using wild-type CPA and CPA_{ST3} as template, respectively, and subcloned into the mammalian expression vector pZ (kindly provided by The Genetics Institute, Cambridge, MA). CPA_{ST3} introduced the decapeptide sequence (-GLSARNRQKR-; Ref. 11) between the prodomain and mature domain of rat CPA (Fig. 1), and CPA_{DAF} fused the 37 amino acid region (-PNKGSQTSGTTRLLSGHTCFTLTGLLGTLVTMGLLT-) from DAF to the COOH terminus of CPA_{ST3} (Ref. 13; see Fig. 6a). All plasmids were confirmed by sequencing at the University of Michigan DNA Sequencing Core.

Cell Culture and Transfections. All cells were cultured under standard conditions in DMEM supplemented with 10% heat-inactivated FBS, penicillin,

streptomycin, and L-glutamine, except for MCF7 cells, which were cultured in RPMI medium with the same supplements. Expression plasmids were transiently transfected into SV40 large T-antigen expressing human embryonic kidney cells (293T) by calcium phosphate precipitation using equal amounts of plasmid DNA for each transfection (10 μ g/ml transfection mixture). To generate CPA for purification, enzymatic assays, or Western blotting, 48 h after transfection plates were washed three times with PBS and then incubated in serum-free medium (Optimem; Life Technologies, Inc., Gaithersburg, MD) for an additional 24 h; at which time the supernatants were harvested, nonadherent cells spun down by centrifugation for 15 min at 1000 \times g, and the conditioned medium frozen at -70°C for subsequent analysis. Stable cell lines expressing CPA_{ST3} were generated by transfecting the CPA_{ST3} expression plasmid or a control plasmid into SCCVII cells using Lipofectamine-PLUS (Life Technologies). Pooled polyclonal transfected cells were then selected for G418 (Life Technologies) resistance for three passages prior to cytotoxicity experiments.

Protein Analysis. For experiments requiring metabolic labeling of proteins, [^{35}S]methionine/cysteine (Pro-mix; Amersham, Arlington Heights, IL) was used according to the protocols described previously (12). Western blotting was performed as described previously (10) using a rabbit polyclonal anti-bovine CPA antisera (Cemicon, Temecula, CA), followed by enhanced chemiluminescence (Pierce, Rockford, IL).

CPA Purification and Enzymatic Assays. CPA was purified from conditioned medium using CPA potato inhibitor affinity chromatography (10) or an α -CPA immunoaffinity column. The α -CPA affinity column was made according to the manufacturer's instructions (Affi-Gel HZ; Bio-Rad, Hercules, CA) using a rabbit α -bovine CPA antibody. Conditioned media were diluted 1:1 with PBS, loaded onto the column, washed (500 mM NaCl in PBS), and eluted (500 mM NaCl, 20 mM Glycine HCl, pH 2.0). Purified CPA was then dialyzed against 500 mM NaCl, 50 mM Tris-HCl (pH 8.0) and stored at 4°C . CPA activity was measured using a spectrophotometric assay for cleavage of a synthetic substrate, N-(3-[2-furyl]acryloyl)-Phe-Phe (Sigma Chemical Co., St. Louis, MO) as described previously (10). Data were plotted, and kinetic constants were calculated by nonlinear regression using GraphPad Prism (GraphPad Software, San Jose, CA).

Retroviral Production and Infection. The cDNAs for CPA_{ST3} or CPA_{DAF} were subcloned into Lzrs.pBMN (kindly provided by Gary Nolan, Stanford, CA), yielding Lz.CPA_{ST3} and Lz.CPA_{DAF}. To generate retroviruses coding for both CPA_{ST3} or CPA_{DAF} and the neomycin resistance gene (*neo*^R) from one bicistronic retrovirus using an IRES, the entire CPA_{ST3}/IRES/*neo*^R or CPA_{DAF}/IRES/*neo*^R expression cassettes were amplified by PCR and subcloned into Lzrs.pBMN, yielding Lz.Neo.CPA_{ST3} and Lz.Neo.CPA_{DAF}. Retroviruses were produced by transfecting the Φ MX-ampho packaging cell line (kindly provided by Gary Nolan, Stanford, CA) using calcium phosphate precipitation, and 48 h after transfection, the producer cells were selected in 0.5 μ g/ml puromycin (Sigma). Retroviral supernatants were generated by plating puromycin-selected producer cells at a density of 40,000 cells/cm² in 100-mm plates and culturing at 32°C for 4 days, with daily harvests. At this time, the supernatants were pooled, filtered through a 0.4 μ m filter, aliquoted, and frozen at -70°C . Cells were infected using retroviral supernatants in the presence of Polybrene (16 μ g/ml; Sigma). The titer of each reach retroviral batch was determined using SCCVII cells and G418 selection for CPA constructs and 5-bromo-4-chloro-3-indolyl- β -D-galactopyranoside staining for β -galactosidase constructs. The titers achieved were $2.4 \times 10^6 \pm 0.7 \times 10^6$, $2.5 \times 10^6 \pm 0.6 \times 10^6$, and $1.1 \times 10^6 \pm 0.3 \times 10^6$ colony-forming units/ml for LacZ, CPA_{ST3}, and CPA_{DAF} respectively.

HPLC Analysis. Tissue culture media were acidified with 1/10th volume 1 M HCl and extracted with -20°C CH₃CN (5:2 CH₃CN:media). Extracts were then analyzed on a C₁₈ reverse phase column (Waters, Milford, MA) by HPLC on a gradient from 10:90:0.1 to 50:90:0.1 CH₃CN:H₂O:trifluoroacetic acid at a flow rate of 1 ml/min over 15 min. HPLC was performed on a Waters gradient system composed of two model 501 pumps, a U6K injector module, and a model 996 photodiode array detector; the system was controlled by Millennium 2010 software. Absorbance was monitored at 315 nm, and under these conditions, MTX had a retention time of 6.4–6.6 min, and MTX-Phe had a retention time of 8.4–8.6 min.

Flow Cytometry. To evaluate cell surface expression of CPA, SCCVII cells were infected with LacZ, CPA_{ST3}, or CPA_{DAF} retrovirus; 48 h later, they were detached from dishes using trypsin, and the trypsin was inactivated by the addition of serum. Cells were then incubated on ice for 30 min in medium

supplemented with a 1:200 dilution of α -CPA antibody. Subsequently, they were centrifuged through a 1/2 ml of FBS to isolate them from unbound antibody and then resuspended in medium supplemented with a 1:200 dilution of R-phycocrythrin conjugated goat α -rabbit IgG secondary antibody (Fischer, Pittsburgh, PA). After 30 min, the unbound antibody was again removed, and the cells were resuspended in PBS for analysis at the University of Michigan Flow Cytometry Core.

Cytotoxicity Assays. For some experiments, growth inhibition was assayed using the sulforhodamine B assay (Sigma; Ref. 16). Cells were plated at a density of 3000 cells/cm² in a 96-well plate; 12–18 h after plating, cells were infected with retroviral supernatants. Twenty-four h after infection, the medium was changed to that supplemented with vehicle (PBS), MTX, or MTX- α -peptides (17). The cells were left cultured with the drug for 72 h, at which point they were fixed and stained according to Skehan *et al.* (16). Data represent the mean \pm SE of at least eight replicate wells. For other experiments, cells were assayed using a CFA (18). Cells were plated in 60-mm dishes at a density of 2000 cells/cm²; 18–24 h later, they were infected with retroviral supernatants for 24 h, at which time the medium was changed to that supplemented with vehicle (PBS), MTX, or MTX-Phe. Cells were cultured with the drug for the indicated time and then plated for colony formation; and after 7–10 days, the dishes were fixed and stained with crystal violet before counting. Data plotted represent the mean and SE of at least three experiments.

CPA Diffusional Assay. To measure the ability of secreted, soluble CPA to sensitize nontransduced cells, a two-chamber tissue culture plate was used. A 50/50 mixture of CPA_{ST3}- or CPA_{DAF}-expressing SCCVII cells and parental SCCVII cells (4000 total) were plated into the top wells of a six-well transwell plate (Costar Transwell-clear; Fischer, Pittsburgh, PA), and at the same time, an equal number (4000 cells) of parental SCCVII cells were plated into the bottom chambers. The top and bottom chambers were separated by a permeable membrane with 0.4 μ m pores such that CPA or small molecules like MTX or MTX-Phe could freely move between the chambers, but whole cells were prohibited from crossing the barrier. The cells were left seeded in the chamber for 48 h, at which time MTX-Phe was added directly to the top and bottom chambers at a uniform concentration of 1 μ M. Both the top and bottom chambers from parallel wells were subsequently trypsinized and plated for CFA at 12-h intervals.

RESULTS

CPA_{ST3} Is Activated by Endogenous Prohormone Convertases. To use CPA in a GDEPT strategy for cancer therapy, we constructed a mutant that is expressed as an active enzyme in the absence of trypsin-dependent propeptide cleavage. Previously, we reported that CPA₉₅, a mutant into which a PC cleavage site was introduced by two amino acid substitutions (FQAR \rightarrow RQKR), is activated but only in the presence of PACE overexpression (Fig. 1; Ref. 10). We, therefore, constructed CPA_{ST3}, which includes a 10-amino acid linker region (-GLSARNRQKR-) between the propeptide and mature domain of CPA (Fig. 1), where the underlined amino acids represent a prototypical PACE/furin cleavage site. This linker region is derived from the matrix-metalloprotease ST3, where it has been demonstrated to sensitize ST3 to PC-dependent activation (11).

To examine the expression and processing of CPA_{ST3}, 293T cells were transiently transfected with the expression plasmids for wild-type CPA, CPA₉₅, or CPA_{ST3} in the absence or presence of a PACE expression plasmid. Conditioned media were collected from transfected cells and analyzed by SDS-PAGE and Western blot. Expression of wild-type CPA alone as well as with cotransfected PACE resulted in a M_r 43,000 protein, which is characteristic of pro-CPA (Fig. 2, Lanes 2 and 3). When CPA₉₅ was expressed in 293T cells, there was a small amount of mature CPA generated, as evidenced by the band at M_r 34,000, yet the majority of the protein was still in the pro- form (Fig. 2, Lane 4). However, in the presence of PACE cotransfection, >50% of CPA₉₅ was processed to the mature form, while the rest remained in the larger pro- form (Fig. 2, Lane 5). These

results are consistent with previous observations for CPA₉₅ when expressed in COS-1 cells and in squamous cell carcinoma lines (10).

In contrast, when CPA_{ST3} was expressed in 293T cells, it was completely processed to the mature form, even in the absence of cotransfected PACE (Fig. 2, Lane 6), and cotransfection of PACE had no impact upon this activation and secretion (Fig. 2, Lane 7). To verify the specificity of this activation, PACE.SA, a dominant-negative mutant of PACE where the active-site serine was mutated to alanine (12), was cotransfected along with CPA_{ST3}. Cotransfection of PACE.SA and CPA_{ST3} inhibited the conversion of CPA_{ST3} from the pro- to mature form (Fig. 2, Lane 8), a further indication that activation of CPA_{ST3} was achieved through the action of endogenous PCs. The observed molecular weights of pro- and mature CPA seen here are consistent with those reported previously for trypsin-activated wild-type CPA (10).

Endogenously Activated CPA_{ST3} Is Indistinguishable from Trypsin-activated Wild-Type CPA. 293T cells were transiently transfected with the CPA_{ST3} expression plasmid, and the protein was purified from the conditioned medium using an anti-CPA immunoaffinity column. Enzymatic analysis using a synthetic substrate, *N*-(3-[2-furyl]acryloyl)-Phe-Phe (1×10^{-5} M to 5×10^{-4} M), demonstrated that endogenously activated CPA_{ST3} had a similar kinetic profile to trypsin-activated wild-type CPA over the range of substrate concentrations studied with K_m and k_{cat} values, which were virtually identical (Table 1). In addition, conditioned medium from 293T cells transiently transfected with CPA_{ST3} was submitted to the University of Michigan Protein Structure Core for electrophoresis and NH₂-terminal sequencing. Ten consecutive amino acids were identified (-ALSTDSFNYA-), which correspond to the first 10 amino acids of mature rat CPA that were immediately COOH-terminal of the PC cleavage site introduced via the ST3 linker region (see Fig. 1; Ref. 19).

Expression of CPA_{ST3} in Squamous Cell Carcinoma Cells Leads to Conversion of MTX-Phe to MTX and Cytotoxicity in a Time-dependent Manner. SCCVII murine squamous cell carcinoma cells were transfected with the pZ.CPA_{ST3} expression plasmid, and a pooled polyclonal CPA_{ST3}-expressing population was selected with G418. The conditioned medium from cells expressing CPA_{ST3} contained CPA, which was predominantly in the mature form, as detected by Western blot and activity assay (data not shown and see Fig. 4a). CPA_{ST3}- or LacZ-expressing cells were exposed to MTX or MTX-Phe for 0–72 h and then plated to determine the SF (Fig. 3a). In addition, at the time of plating conditioned media were collected for analysis by HPLC (Fig. 3b). When either LacZ- or CPA_{ST3}-expressing cells were exposed to 1 μ M MTX, there was significant cytotoxicity observed starting 12 h after exposure, which peaked at a SF of <0.001 after 36–48 h (Fig. 3a). However, there was no apparent cytotoxicity to LacZ-expressing cells exposed to 1 μ M MTX-Phe for 72 h with a SF > 0.9 (Fig. 3a) and no detectable conversion of MTX-Phe to MTX (data not shown). In contrast, CPA_{ST3}-expressing cells were potentially sensitized to MTX-Phe; this cytotoxicity approached that of MTX, reaching a SF of slightly >0.001 after 72 h of exposure to 1 μ M MTX-Phe (Fig. 3a).

The time course of cytotoxicity for MTX-Phe in CPA-expressing cells was somewhat delayed when compared with MTX toxicity; however, because the CPA in the culture medium was removed when the medium was replaced with fresh medium containing MTX-Phe, this delay in cytotoxicity was probably attributable to the time needed for the cells to synthesize fresh CPA. Indeed, the delayed cytotoxicity directly correlated with the production of MTX in the tissue culture medium, as determined by HPLC (Fig. 3b). Furthermore, the addition of MTX-Phe directly to the culture without changing the medium

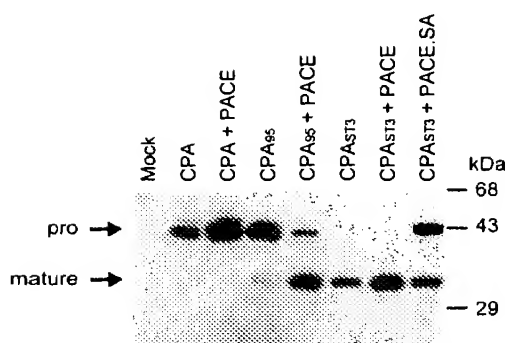


Fig. 2. Expression of CPA_{ST3} results in mature CPA in the absence of PACE coexpression. Expression plasmids for wild-type, CPA_{ST3}, and CPA_{ST3} constructs were transfected into 293T cells either alone or in cotransfection with PACE or dominant-negative PACE (PACE.SA). A total of 5 μ g of the different CPA expression plasmids were used in each condition supplement with 5 μ g of the PACE constructs or empty vector. Forty-eight h after transfection, conditioned media were harvested and analyzed by SDS-PAGE and Western blot analysis using a CPA-specific polyclonal antibody. Arrows, pro and mature forms of CPA. As a control, 293T cells were transfected in the absence of DNA and analyzed as above (Mock).

Table 1 Kinetic analysis of wild-type CPA and CPA_{ST3}

Hydrolysis of *N*-(3-[2-furyl]acryloyl)-Phe-Phe by 2.0×10^{-10} mol trypsin-activated CPA or endogenously activated CPA_{ST3} was monitored at 330 nm in assay buffer (pH 7.5; 50 mM Tris-HCl, 0.45 M NaCl; 25°C). Kinetic constants were calculated by nonlinear regression and are given as the mean of three trials \pm SE.

Enzyme	K_m (mM)	k_{cat} (1/min)
CPA	$7.8 \times 10^{-2} \pm 9.2 \times 10^{-3}$	$13,000 \pm 725$
CPA _{ST3}	$8.2 \times 10^{-2} \pm 9.6 \times 10^{-3}$	$12,250 \pm 1,135$

shifted the time course of sensitization such that it more closely paralleled that of MTX (data not shown).

Retroviral Transduction of Tumor Cell Lines Leads to Production of Mature CPA and Sensitivity to MTX-Phe. Because the use of stable cell lines may not accurately represent a gene therapy strategy, a CPA_{ST3} retrovirus was produced by subcloning the CPA_{ST3} cDNA into the LacZ.pBMN expression plasmid and transfecting the Φ Nx retroviral producer line. A Western blot of the conditioned medium from this retroviral producer line indicated that these cells secrete mature CPA_{ST3} (Fig. 4a). Three tumor cell lines, SCCVII murine squamous cell carcinoma, UMSCC6 human squamous cell carcinoma, and MCF7 human breast carcinoma, were infected with either CPA_{ST3}- or LacZ-expressing retrovirus. LacZ infection, followed by β -galactosidase staining, revealed that \sim 50% of SCCVII cells were infected, whereas for the other two cell lines, the infection rate was \sim 25–30% (data not shown). Forty-eight h after infection, the cells were labeled with [³⁵S]methionine/cysteine for 30 min, followed by a 4-h chase, and the conditioned media were immunoprecipitated using an α -CPA antibody and then analyzed by SDS-PAGE and autoradiography. Cells infected with LacZ virus did not produce any detectable CPA; however, cells infected with the CPA_{ST3} retrovirus produced CPA that was predominantly in the mature form, as evidenced by the band at M_r 34,000 (Fig. 4a). In addition, in a parallel series of plates, infected cells were exposed to 1 μ M MTX-Phe for 72 h before plating to analyze their SF. For all three lines tested, LacZ-infected cells were resistant to MTX-Phe (SF > 0.75), whereas CPA_{ST3}-infected cells were potently sensitized to the prodrug (SF of 0.01 to 0.00 liter).

CPA_{ST3}-expressing Cells Are Sensitized to MTX-Phe in a Dose-dependent Manner. More detailed studies on prodrug activation by CPA_{ST3} were performed using SCCVII cells at a range of MTX and

MTX-Phe concentrations from 1 to 1000 nM. Both LacZ- and CPA_{ST3}-expressing cells were sensitive to MTX exhibiting a SF of 0.001 at 1000 nM MTX and IC₅₀ and IC₉₅ values of 1 and 25 nM, respectively (Fig. 5 and Table 2). There was no toxicity to LacZ-infected cultures, even when exposed to 1000 nM MTX-Phe (Fig. 5 and Table 2). However, infection of SCCVII cells with CPA_{ST3} retrovirus, followed by exposure to MTX-Phe, resulted in cytotoxicity in a dose-dependent manner that paralleled that of MTX exhibiting a SF of about 0.001 at 1000 nM MTX-Phe and IC₅₀ and IC₉₅ values of 2.5 and 35 nM, respectively (Fig. 5 and Table 2).

Construction and Characterization of a Cell Surface Form of CPA. The GDEPT strategy for cancer therapy described here relies upon the extracellular secretion of soluble active CPA, which can then cleave the prodrug MTX-Phe, yielding MTX. However, release of a secreted and diffusible form of CPA into the extracellular space in an *in vivo* model has the potential to result in both decreased tumoral cytotoxicity and also systemic toxicity. To alleviate these limitations, we constructed a modified form of CPA_{ST3} wherein the COOH terminus of DAF was fused to CPA_{ST3}, and the molecule thus was linked to the cell surface by a glycopospholipid linkage (Fig. 6a).

Both the soluble (CPA_{ST3}) and the cell-surface tethered form (CPA_{DAF}) of CPA were transiently expressed in 293T cells; 48 h after transfection, the cells were labeled with [³⁵S]methionine/cysteine for 10 min, and cell extracts were collected. In parallel plates, labeled cells were chased in serum-free medium for 5 h prior to the collection of both cell extracts and conditioned medium. Cell lysates from both the early and late time points were then lysed in a Dounce homogenizer and submitted to a 100,000 \times g spin to precipitate cellular

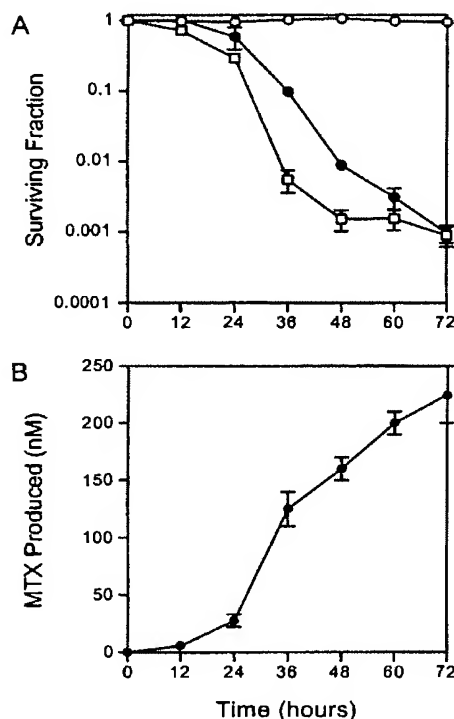


Fig. 3. CPA_{ST3}-expressing cells convert MTX-Phe to MTX and are sensitized to the prodrug in a time-dependent manner. SCCVII cells expressing LacZ or CPA_{ST3} were exposed to MTX or MTX-Phe for 0–72 h and then evaluated by CFA (A), and HPLC analysis was performed on the condition media at the time of plating (B). LacZ-expressing cells treated with MTX (□) or MTX-Phe (○) and CPA_{ST3}-expressing cells exposed to MTX-Phe (●) are shown.

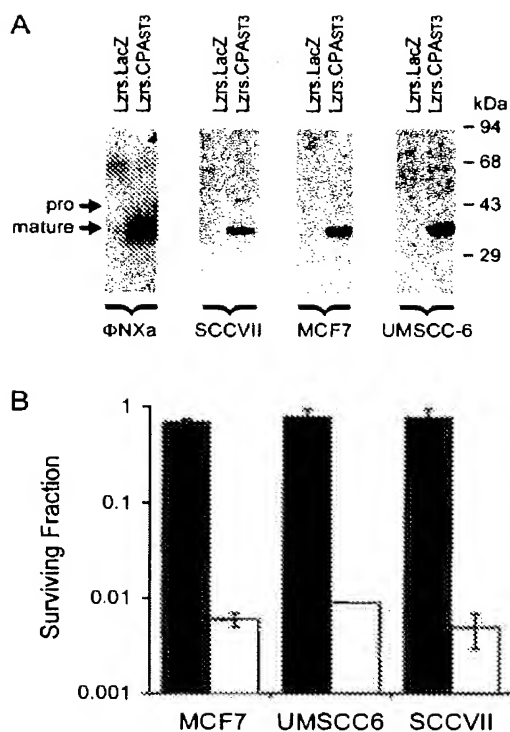


Fig. 4. Retroviral infection with CPA_{ST3} results in secretion of mature CPA and sensitization to MTX-Phe. The supernatants from Lzr.LacZ or Lzr.CPA_{ST3} retroviral producer cells were analyzed by SDS-PAGE and Western blotting for CPA expression (A, leftmost panel). Three tumor cell lines (SCCVII, MCF7, and UMSCC6) were infected with LacZ or CPA_{ST3} retrovirus, metabolically labeled with [³⁵S]methionine/cysteine, and conditioned media were analyzed by immunoprecipitation, SDS-PAGE, and autoradiography (A, right three panels). Arrows, pro and mature forms of CPA. In parallel cultures, LacZ or CPA_{ST3}-infected cells were treated with MTX-Phe for 48 h and plated for surviving fraction (B). Bars, SE.

membranes (S100). The S100 fractions as well as the conditioned medium were analyzed by immunoprecipitation, followed by SDS-PAGE and autoradiography. CPA_{ST3} was initially synthesized as a M_r 43,000 pro-form and subsequently converted to the M_r 34,000 mature form and secreted from the cell such that after a 5-h chase, it accumulated in the conditioned medium and was no longer detectable in the cell extract (Fig. 6b). In contrast, CPA_{DAF} was initially synthesized as a M_r 48,000 form and then converted to a M_r 38,000 form, which remained cell associated and was undetectable in the conditioned medium (Fig. 6b), thus indicating that CPA_{DAF} is cell associated whereas CPA_{ST3} is secreted.

In a separate experiment, 293T cells were mock-transfected or transfected with either CPA_{ST3} or CPA_{DAF}. Conditioned medium and S100 fractions were collected from the transfected plates and assayed for CPA activity. The S100 cell pellet from mock or CPA_{ST3}-transfected cells had little or no catalytic activity, whereas the S100 fraction from CPA_{DAF} transfected cells rapidly cleaved the synthetic substrate (data not shown). Finally, unlike CPA_{ST3} which contained significant catalytic activity in the conditioned medium, such activity was undetectable in the conditioned medium derived from mock or CPA_{DAF}-transfected cells (data not shown).

To further verify that CPA_{DAF} was expressed on the cell surface, a CPA_{DAF} retrovirus was generated by subcloning the cDNA for CPA_{DAF} into Laz.pBMN. SCCVII cells were infected with LacZ, CPA_{ST3}, or CPA_{DAF} virus, and 48 h after infection, they were analyzed for cell surface expression of CPA by flow cytometry. Cells

infected with CPA_{DAF} had a >100-fold increase in staining using an anti-CPA antibody when compared with LacZ- or CPA_{ST3}-infected cells, thus demonstrating that not only is CPA_{DAF} cell associated, but it is also cell-surface exposed (Fig. 6c).

To evaluate whether the CPA_{DAF} molecule retained a substrate specificity similar to the native enzyme, we performed sulforhodamine B growth inhibition assays using five different MTX- α -peptides (17) to compare the substrate specificity of CPA_{ST3} and CPA_{DAF}, as measured by their ability to sensitize cells to these prodrugs using the sulforhodamine B growth inhibition assay (Table 3). Both CPA_{ST3} and CPA_{DAF} showed a preference for the large aromatic side chain prodrugs, with MTX-Phe being the best used substrate, followed by MTX-Tyr. Both forms of CPA had slight activity against MTX-Met with little or no activity *versus* MTX-Gln and MTX-Trp. Although the trend of substrate specificity was consistent between CPA_{ST3} and CPA_{DAF}, the absolute level of activity varied with CPA_{ST3} consistently having greater activity than CPA_{DAF}; however, this difference may not reflect actual differences in activity and instead most likely is an indication of different titers of retroviruses (see below).

CPA_{ST3} and CPA_{DAF} Both Exhibit a Potent Bystander Effect. In any cancer gene therapy strategy, only a small portion of the tumor can normally be transduced, typically <10% of the total tumor mass. Therefore, the ability of transduced cells to kill both transduced and nontransduced cells is an important aspect of a GDEPT strategy. To evaluate the potential bystander effect of the system described herein, retroviral constructs were generated where either CPA_{ST3} or CPA_{DAF} are expressed from the same bicistronic mRNA as the neomycin resistance gene (*neo^R*), thus enabling one to select and quantify infected cells based upon resistance to G418. SCCVII cells were infected with titers of Lz.Neo.CPA_{ST3} or Lz.Neo.CPA_{DAF} retrovirus ranging from 1.25×10^4 to 1.0×10^6 colony-forming units/ml in a series of parallel dishes. In one pair of dishes, cells infected at increasing titers of virus were plated at varying dilutions with and without G418

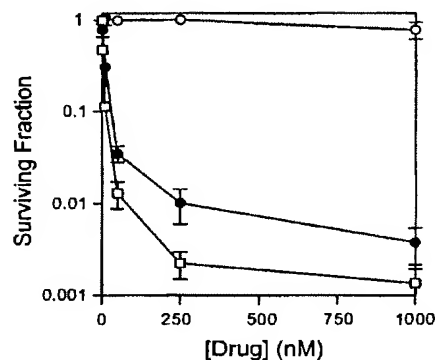


Fig. 5. Retroviral infection with CPA_{ST3} sensitizes cells to MTX-Phe in a dose-dependent manner. SCCVII cells were infected with LacZ or CPA_{ST3} retrovirus and then treated with increasing doses of MTX or MTX-Phe for 48 h prior to plating for SF. CPA_{ST3}-infected cells treated with MTX (□), LacZ-infected cells treated with MTX-Phe (○), and CPA_{ST3}-infected cells treated with MTX-Phe (●) are shown. Bars, SE.

Table 2 Retroviral transduction sensitizes cells to MTX-Phe

SCCVII cells were infected with CPA_{ST3} or LacZ retrovirus, treated with MTX or MTX-Phe for 48 h, and then assayed by colony formation. Data represent the mean \pm SE of three experiments.

Drug (nM)	MTX	MTX-Phe	
		LacZ	CPA _{ST3}
IC ₅₀	1.1 \pm 0.2	>1000	2.5 \pm 1.9
IC ₉₅	25.3 \pm 4.7	>1000	34.0 \pm 5.3

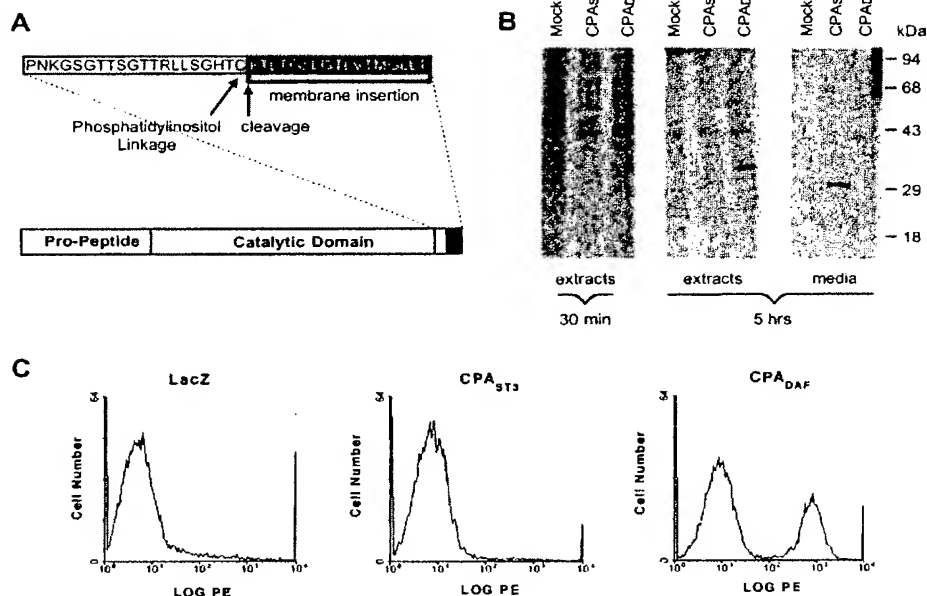


Fig. 6. Expression of CPA_{DAF} results in cell surface-localized CPA without release into the conditioned medium. CPA_{DAF} was constructed by fusing the 37-amino acid glycopospholipid membrane anchoring domain from DAF to the COOH-terminus of CPA (A). 293T cells were mock transfected or transfected with CPA_{ST3} or CPA_{DAF}, and cell extracts or conditioned media were then analyzed by immunoprecipitation, SDS-PAGE, and autoradiography after a 30-min pulse with [³⁵S]cysteine/methionine or after a 30-min pulse, followed by a 5-h chase (B). SCCVII cells were infected with LacZ, CPA_{ST3}, or CPA_{DAF} and then analyzed for cell surface expression of CPA by flow cytometry (C).

selection (400 μ g/ml), and the number of G418-resistant colonies was used to calculate the "% infected cells" for each viral titer. In the second pair of dishes, cells infected at the same viral titers were treated with 1 μ M MTX-Phe for 48 h, at which time they were plated and the SF subsequently calculated. These data were plotted as "surviving fraction" as a function of "% infected cells" (Fig. 7). In addition, to verify these infection rates, the cell surface construct was also assayed by flow cytometric analysis, which gave results consistent with G418 selection (data not shown).

When cultures were infected with varying dilutions of virus and then treated with MTX-Phe, the CPA_{DAF}-infected cultures were more sensitized to the drug than the CPA_{ST3}-infected cultures, even at equal rates of infectivity (Fig. 7). A culture of ~50% CPA_{DAF}-expressing cells exhibited a SF of <0.001 in the presence of 1 μ M MTX-Phe, and the level of cytotoxicity decreased as the percentage of infected cells decreased to a SF of <0.1 at 5% CPA_{DAF} expression. CPA_{ST3}, in contrast, peaked at a SF of slightly >0.001 for a 50% expressing culture, and there was little cytotoxicity seen below a 10% expressing culture (SF > 0.75).

CPA_{DAF} Partially Protects from Collateral Cytotoxicity. Finally, to determine whether the release of secreted CPA_{ST3} would sensitize cells distant from the site of production, a unique coculture assay was developed to measure the impact of the diffusion of CPA_{ST3} on the cytotoxicity of nontransduced cells located some distance from the CPA-expressing cells. SCCVII cells that were 50% CPA_{ST3} or 50% CPA_{DAF} expressing were plated in the top chambers of a two-chamber, six-well tissue culture plate, and an equal number of nontransduced SCCVII cells were plated in the bottom chamber. The membrane dividing the two chambers had a 0.4 μ m pore size, which was small enough to prohibit the passage of whole cells between the chambers; however, released CPA_{ST3} and both MTX-Phe and MTX would readily diffuse between the chambers. The seeded cells were left in culture for 48 h, at which point MTX-Phe was added to the medium in both the top and bottom chambers to a final concentration of 1 μ M, and the cells were plated for CFA at 12-h intervals.

Consistent with previous results, nontransduced parental cells exhibited no toxicity when exposed to the prodrug (Fig. 8). However, for CPA_{ST3}- and CPA_{DAF}-expressing cultures, cytotoxicity was observed for both the transduced wells (the top chamber) and the bystander cells (the bottom chamber). The toxicity appeared first in the top chambers and increased with the time of exposure to the prodrug. The level and rate of cytotoxicity in the top chambers was similar between CPA_{ST3} and CPA_{DAF} cultures throughout the course of the experiment (Fig. 8). However, there was a difference in collateral cytotoxicity to cells in the lower chambers, with cytotoxicity apparent earlier and to a greater extent in CPA_{ST3} cultures than in CPA_{DAF} cultures (Fig. 8). Therefore, the anchoring of CPA_{DAF} to the surface of the cell conferred potent sensitization to both CPA_{DAF}-expressing and bystander cells in close proximity to each other (those in the top chamber) in a manner similar to CPA_{ST3}-expressing cells. Yet, although there was collateral cytotoxicity to cells some distance from the CPA_{DAF}-expressing cells (those in the bottom chamber), this cytotoxicity appeared later and to a lesser extent than that seen for CPA_{ST3}-expressing cells, where the enzyme could diffuse into the lower chamber and generate MTX *in situ*.

DISCUSSION

GDEPT strategies have been proposed as a means of achieving high intratumoral levels of chemotherapeutics with decreased systemic toxicity. The best studied of these include the HSV-TK/ganciclovir (20) and the CD/5-FC systems (21). One common feature of these systems is their reliance upon nonmammalian enzymes that therefore are highly immunogenic. Although the added immune response may contribute to the antitumoral effect (2), the destruction of transduced cells by the host immune system could also inhibit the efficacy of repetitive prodrug administration. The system detailed here is appealing in that it relies upon a mammalian enzyme that is highly conserved and therefore should be only mildly immunogenic; thus repetitive or long-term prodrug administration may be possible.

In addition, for both the HSV-TK/ganciclovir and the CD/5-FC

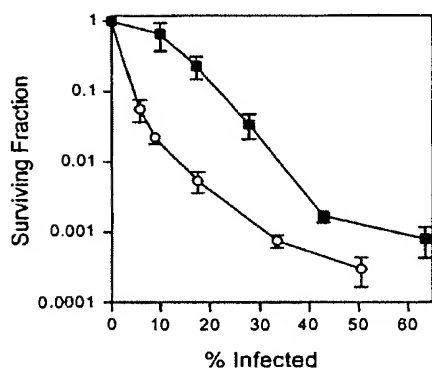


Fig. 7. CPA_{ST3}- and CPA_{DAF}-expressing cells both exhibit a potent bystander effect. SCCVII cells were infected with increasing dilutions of CPA_{ST3} or CPA_{DAF} retrovirus and plated for colony formation in the absence or presence of G418 to determine percentage of infected cells. In parallel plates, CPA_{ST3} (■) or CPA_{DAF} (○) infected cells were treated with MTX-Phe for 48 h before plating for SF. Bars, SE.

systems, it has been demonstrated that the "factory" or transduced cells are killed earlier and at lower doses of prodrug than nontransduced cells because of the intracellular accumulation of the toxic metabolites (22–26). In the case of HSV-TK/ganciclovir, this results in very little cytotoxicity when <50% of the cells in culture are expressing HSV-TK. Because of the fact that 5-fluorouracil is membrane permeable, there is a greater bystander effect for the CD/5-FC system. Unfortunately, we still have witnessed limited cytotoxicity with a low percentage of CD expressing cells both in culture (25) and in animal models (26). In the GDEPT reported here, extracellular production of MTX by soluble or cell surface CPA should equally sensitize both transduced and bystander cells with minimal preferential cytotoxicity.

One additional advantage of this system is that because MTX is one of the most widely used agents in the treatment of solid tumors, its pharmacokinetics, dose-limiting toxicities, and mechanisms of resistance are well understood (3, 4). HD-MTX therapy has been suggested as a means to circumvent tumor-derived resistance to MTX and is used quite commonly in current oncological practice. Recently, other strategies have been developed to genetically modify bone marrow stem cells to make them resistant to MTX so that HD-MTX treatment could be undertaken while biochemically protecting the bone marrow. These protective strategies have been demonstrated both for human bone marrow in culture (27) and for the protection of mice from MTX toxicity after transplantation of MTX-resistant bone marrow (28). Although these strategies have provided promising results, they do not offer any protection to the gastrointestinal tract, which is also highly sensitive to MTX-induced toxicity. The GDEPT proposed here by localizing HD-MTX to the tumor site may be able to increase the cytotoxic dose delivered to the tumor while protecting both the gastrointestinal tract and the bone marrow. An additional advantage for the use of CPA in an enzyme/prodrug strategy is that other antifolates, which have proven cytotoxic even in MTX-resistant cell lines (29), also rely upon transport through the reduced folate carrier. Therefore, these drugs could be converted to α -peptide blocked prodrugs to be used in this enzyme/prodrug strategy (30, 31).

To render CPA active in the absence of trypsin-dependent zymogen cleavage, the 10-amino acid linker region from ST3 was incorporated into CPA between the pro- and mature domains such that if cleavage occurred at the expected site, the mature peptide released would be identical to trypsin-activated CPA. Enzymatic analysis of purified CPA_{ST3} confirmed the correct activation of the zymogen to the catalytic form for its kinetic profile was indistinguishable from the

trypsin-activated CPA. NH₂-terminal sequencing of endogenously activated CPA_{ST3} also revealed that cleavage occurred at the expected location, liberating a mature peptide that is identical to the native mature protein. This is the first direct biochemical demonstration of the cleavage site for the ST3 linker region; the work that identified this cleavage domain was based upon site-directed mutagenesis to indirectly ascertain which site was cleaved (11).

CPA_{ST3}-transduced squamous cell carcinoma cells were able to generate MTX from MTX-Phe. Further evidence for the specificity of this activation was demonstrated by the inhibition of the conversion by the carboxypeptidase inhibitor derived from potatoes (data not shown). MTX was first detected 12 h after exposure to the prodrug, and by 72 h, >200 nM MTX was generated. Although this only amounted to a 20% conversion of MTX-Phe to MTX, the amount of MTX generated was still almost 10 times higher than the IC₉₅ of MTX in this cell line and thus was more than sufficient to cause potent cytotoxicity (see Table 2). These data are consistent with the notion that the MTX generated within the first 24 h inhibited cellular growth and the further production of CPA and, therefore, limited the final conversion of MTX-Phe to MTX. However, this MTX-mediated inhibition of further CPA production has not been proven.

Having ascertained that secreted active CPA_{ST3} could indeed sensitize a number of different tumor cell lines to MTX-Phe after retroviral infection, we next developed a cell surface-associated form of endogenously active CPA. Unlike previous reports where carboxypeptidase G2 was still highly active both *in vitro* and *in vivo* when fused to the transmembrane domain of a cell surface receptor (32), we were unable to detect any functional CPA after construction of a similar fusion protein with CPA (data not shown). However, the use of the phospholipid membrane anchor from DAF resulted in a CPA molecule that not only remained cell tethered but was also functional, perhaps because of the increased conformational flexibility allowed by the lipid linkage as compared with a more rigid peptide transmembrane domain. This molecule, CPA_{DAF}, was able to sensitize SCCVII cells to MTX-Phe in a manner similar to the secreted form, and it appears to have retained the substrate specificity of the native molecule.

CPA_{DAF} also sensitized SCCVII cells to MTX-Phe when only a very small fraction of cells (~5%) were expressing the protein. This may be attributable to the fact that time is not necessary for the molecule to build-up in the culture medium, because CPA_{DAF} is anchored to the surface of the cell and does not diffuse away, and thus it is not removed when the culture medium is changed. The heightened cytotoxicity of CPA_{DAF} when compared with CPA_{ST3} also may be attributable to the local production of MTX at the cell surface, thus requiring lower total conversion levels of MTX-Phe to MTX to sensitize cells. This theory has been suggested for ADEPT protocols using CPA. Kuefner *et al.* (5) determined that when using antibody-conjugated CPA localized to the surface of the cell, 100-fold less enzyme was required to achieve equal sensitization as that found when purified CPA was simply added to the culture medium. They attributed this enhanced cytotoxicity to the production of MTX within

Table 3. Retroviral transduction with CPA_{ST3} or CPA_{DAF} sensitizes cells to MTX- α -peptide prodrugs

The IC₅₀s of five MTX- α -peptide prodrugs were evaluated using a 96-well plate growth inhibition assay after retroviral transduction of SCCVII cells with LacZ, CPA_{ST3}, or CPA_{DAF} retrovirus. Data represent the average of at least eight replicate wells.

MTX- α -peptide	LacZ	CPA _{ST3}	CPA _{DAF}
Trp	4000	4000	4000
Gln	3000	2000	3000
Met	6000	2000	3000
Tyr	5000	450	1000
Phe	15,000	200	500

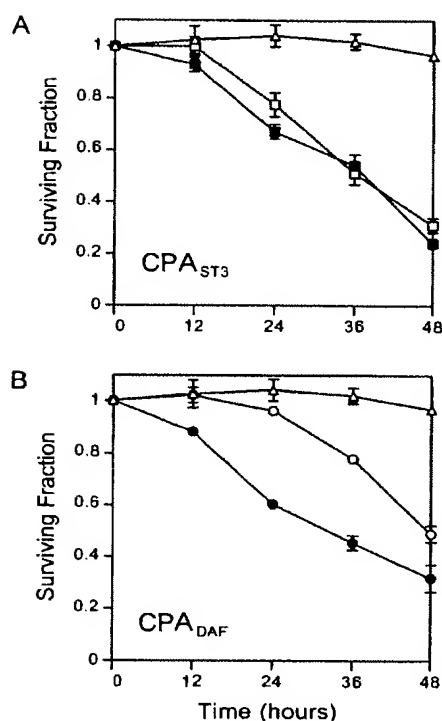


Fig. 8. CPA_{DAF} expression sensitizes infected and "bystander cells" to MTX-Phe while exhibiting reduced collateral toxicity. CPA_{ST3}- or CPA_{DAF}-expressing SCCVII cells were mixed at a 50:50 ratio with parental SCCVII cells and plated in the top of a dual chamber tissue culture plate. In the bottom chamber, an equal number of parental SCCVII cells were plated. Both chambers were then treated with 1 μ M MTX-Phe, and parallel wells were plated for SF at 12-h intervals. Parental cells alone exposed to MTX-Phe (Δ), cells from the top culture (\blacksquare , \bullet), or cells from the bottom culture (\square , \circ) are shown. A. CPA_{ST3} cocultures (\square , \blacksquare). Bars, SE. B. CPA_{DAF} cocultures (\circ , \bullet). Bars, SE.

the microenvironment around cell surface-localized CPA-antibody conjugates. In addition, by prohibiting the diffusion of the catalytically active enzyme away from transduced cells, CPA_{DAF} also partially inhibited collateral toxicity to cells more distant from the site of enzyme production than that seen for CPA_{ST3}, a fact that may be more readily apparent and more critical when this strategy is evaluated *in vivo*.

The studies reported here have focused on MTX-Phe, because it was identified as the best substrate for wild-type CPA (17). However, it has recently been demonstrated that this compound, unlike predictions, is not stable *in vivo* for it is rapidly converted to MTX after injection into mice, which prohibits direct evaluation of this GDEPT in an animal model (8). To overcome the unsuitability of MTX-Phe, modified MTX- α -peptide prodrugs with nonnatural amino acid blocking groups have been described that are poor substrates for endogenous systemic CPA-like activities and are thus highly stable *in vivo*. For example, the MTX-3-cyclopentyl-Tyr prodrug is 50,000-fold more stable in the presence of wild-type CPA than MTX-Phe (8). In addition, although these compounds are poor substrates for wild-type CPA, they are efficiently cleaved by the T268G mutant of CPA, which has an alteration in the substrate binding pocket. The efficacy of the endogenously active soluble (CPA_{ST3}) and cell surface forms of CPA (CPA_{DAF}) when combined with the T268G altered specificity form of the enzyme are now being evaluated. Preliminary evidence, which is in accordance with Smith *et al.* (8), suggests that expression of this T268G mutant in culture confers sensitization to MTX-3-

cyclopentyl-Tyr, whereas expression of the wild-type enzyme has no such capacity.

Recently, studies using the T268G mutant of human CPA in an ADEPT protocol were unable to demonstrate a clinical response because of the rapid inactivation of CPA *in vivo* (31). To allow time for distribution, binding, and subsequent clearance of unbound CPA/antibody conjugates, the authors waited 24 h after injection before they initiated prodrug treatment. However, the half-life of the enzyme/antibody conjugate *in vivo* was found to be significantly less than this, and as a result, there was little conversion of MTX-prodrugs. The CPA GDEPT strategy described here may circumvent this limitation through the continuous production of CPA by virally transduced cells, thus limiting the impact of protein inactivation. Because of the clinical efficacy of MTX in the treatment of squamous cell cancer of the head and neck and to the difficulty in achieving local control of head and neck cancer (33), future studies will be focused on the use of this GDEPT in the treatment of head and neck cancer by direct injection of CPA_{ST3}- or CPA_{DAF}-expressing adenoviruses into submental tumors in an animal model of head and neck cancer (26, 34, 35).

ACKNOWLEDGMENTS

We thank Leo Ostruszka and Donna Shewach for assistance with HPLC analysis of MTX and MTX-Phe. We also thank Amy Pace for excellent help with graphic arts.

REFERENCES

- Krakoff, I. The irrelevant toxicities of anticancer drugs. In: M. Hacker, J. Lazo, and T. Tritton (eds.), *Organ Directed Toxicities of Anticancer Drugs*, pp. 3-12. Boston: Martinus Nijhoff, 1987.
- Niculescu-Duvaz, I., Spooner, R., Marais, R., and Springer, C. J. Gene-directed enzyme prodrug therapy. *Bioconj. Chem.*, 9: 4-22, 1998.
- Tattersall, M. Clinical utility of methotrexate in neoplastic disease. In: F. Siotnak, J. Burchall, W. Ensinger, and J. Montgomery (eds.), *Folate Antagonists as Therapeutic Agents*, Vol. 2, pp. 166-189. Orlando: Academic Press, 1984.
- Ensinger, W. Clinical pharmacology of folate analogs. In: F. Siotnak, J. Burchall, W. Ensinger, and J. Montgomery (eds.), *Folate Antagonists as Therapeutic Agents*, Vol. 2, pp. 133-159. Orlando: Academic Press, 1984.
- Kuefner, U., Lohmann, U., Montejano, Y. D., Vitols, K. S., and Huennekens, F. M. Carboxypeptidase-mediated release of methotrexate from methotrexate α -peptides. *Biochemistry*, 28: 2288-2297, 1989.
- Oppezzo, O., Ventura, S., Bergman, T., Vendrell, J., Jorvall, H., and Aviles, F. X. Procarboxypeptidase in rat pancreas. Overall characterization and comparison of the activation processes. *Eur. J. Biochem.*, 222: 55-63, 1994.
- Perron, M. J., and Page, M. Activation of methotrexate-phenylalanine by monoclonal antibody-carboxypeptidase A conjugate for the specific treatment of ovarian cancer *in vitro*. *Br. J. Cancer*, 73: 281-287, 1996.
- Smith, G. K., Banks, S., Blumenkopf, T. A., Cory, M., Humphreys, J., Laethem, R. M., Miller, J., Moxham, C. P., Mullin, R., Ray, P. H., Walton, L. M., and Wolfe, L. A., III. Toward antibody-directed enzyme prodrug therapy with the T268G mutant of human carboxypeptidase A1 and novel *in vivo* stable prodrugs of methotrexate. *J. Biol. Chem.*, 272: 15804-15816, 1997.
- Nakayama, K. Furin: a mammalian subtilisin/Kex2p-like endoprotease involved in processing of a wide variety of precursor proteins. *Biochem. J.*, 327: 625-635, 1997.
- Hamstra, D. A., and Rehemtulla, A. Toward an enzyme/prodrug strategy for cancer gene therapy: endogenous activation of carboxypeptidase A mutants by the PACE/Furin family of propeptidases. *Hum. Gene Ther.*, 10: 235-248, 1999.
- Pei, D., and Weiss, S. J. Furin-dependent intracellular activation of the human stromelysin-3 zymogen. *Nature (Lond.)*, 375: 244-247, 1995.
- Rehemtulla, A., and Kaufman, R. J. Preferred sequence requirements for cleavage of pro-von Willebrand factor by propeptide-processing enzymes. *Blood*, 79: 2349-2355, 1992.
- Caras, I. W., Weddell, G. N., Davitz, M. A., Nussenzweig, V., and Martin, D. W., Jr. Signal for attachment of a phospholipid membrane anchor in decay accelerating factor. *Science (Washington DC)*, 238: 1280-1283, 1987.
- Sambrook, J., Fritsch, E., and Maniatis, T. *Molecular Cloning: A Laboratory Manual*, Ed. 2. Cold Springs Harbor, NY: Cold Springs Harbor Laboratory, 1989.
- Hugachi, R. Recombinant PCR. In: M. Innis, D. Gelfand, J. Snisky, and T. White (eds.), *PCR Protocols: A Guide to Methods and Applications*, pp. 177-183. San Diego: Academic Press, 1990.
- Skehan, P., Storeng, R., Scudiero, D., Monks, A., McMahon, J., Vistica, D., Warren, J. T., Bokesch, H., Kenney, S., and Boyd, M. R. New colorimetric cytotoxicity assay for anticancer-drug screening. *J. Natl. Cancer Inst.*, 82: 1107-1112, 1990.
- Perron, M.-J., and Page, M. Synthesis of methotrexate prodrugs as an approach for drug targeting. *Int. J. Oncol.*, 5: 907-913, 1994.

18. Rehemtulla, A., Hamilton, C. A., Chinnaiyan, A. M., and Dixit, V. M. Ultraviolet radiation-induced apoptosis is mediated by activation of CD-95 (Fas/APO-1). *J. Biol. Chem.*, 272: 25783-25786, 1997.
19. Quinto, C., Quiroga, M., Swain, W. F., Nikovits, W. C., Jr., Standing, D. N., Pictet, R. L., Valenzuela, P., and Rutter, W. J. Rat preprocarboxypeptidase A: cDNA sequence and preliminary characterization of the gene. *Proc. Natl. Acad. Sci. USA*, 79: 31-35, 1982.
20. Moolten, F. L. Tumor chemosensitivity conferred by inserted herpes thymidine kinase genes: paradigm for a prospective cancer control strategy. *Cancer Res.*, 46: 5276-5281, 1986.
21. Huber, B. E., Richards, C. A., and Krenitsky, T. A. Retroviral-mediated gene therapy for the treatment of hepatocellular carcinoma: an innovative approach for cancer therapy. *Proc. Natl. Acad. Sci. USA*, 88: 8039-8043, 1991.
22. Fick, J., Barker, F. G., II, Dazin, P., Westphale, E. M., Beyer, E. C., and Israel, M. A. The extent of heterocellular communication mediated by gap junctions is predictive of bystander tumor cytotoxicity *in vitro*. *Proc. Natl. Acad. Sci. USA*, 92: 11071-11075, 1995.
23. Mesnil, M., Piccoli, C., Tiraby, G., Willecke, K., and Yamasaki, H. Bystander killing of cancer cells by herpes simplex virus thymidine kinase gene is mediated by connexins. *Proc. Natl. Acad. Sci. USA*, 93: 1831-1835, 1996.
24. Wygoda, M. R., Wilson, M. R., Davis, M. A., Trosko, J. E., Rehemtulla, A., and Lawrence, T. S. Protection of herpes simplex virus thymidine kinase-transduced cells from ganciclovir-mediated cytotoxicity by bystander cells: the Good Samaritan effect. *Cancer Res.*, 57: 1699-1703, 1997.
25. Lawrence, T. S., Rehemtulla, A., Ng, E. Y., Wilson, M., Trosko, J. E., and Stetson, P. L. Preferential cytotoxicity of cells transduced with cytosine deaminase compared to bystander cells after treatment with 5-fluorocytosine. *Cancer Res.*, 58: 2588-2593, 1998.
26. Hamstra, D. H., Rice, D. J., Pu, A., Oyedijo, D., Ross, B. D., and Rehemtulla, A. Combined radiation and enzyme/prodrug therapy for head and neck cancer in an orthotopic. *Anim. Model Rad. Res.*, in press, 2000.
27. Hock, R. A., and Miller, A. D. Retrovirus-mediated transfer and expression of drug resistance genes in haematopoietic progenitor cells. *Nature (Lond.)*, 320: 275-277, 1986.
28. Williams, D. A., Hsieh, K., DeSilva, A., and Mulligan, R. C. Protection of bone marrow transplant recipients from lethal doses of methotrexate by the generation of methotrexate-resistant bone marrow. *J. Exp. Med.*, 166: 210-218, 1987.
29. Li, W. W., Tong, W. P., and Bertino, J. Antitumor activity of antifolate inhibitors of thymidylate and purine synthesis in human soft tissue sarcoma lines with intrinsic resistance to methotrexate. *Clin. Cancer Res.*, 10: 631-636, 1995.
30. Springer, C. J., Bavetsias, V., Jackman, A. L., Boyle, F. T., Marshall, D., Pedley, R. B., and Bisset, G. M. Prodrugs of thymidylate synthase inhibitors: potential for antibody directed enzyme prodrug therapy (ADEPT). *Anti-Cancer Drug Des.*, 11: 625-636, 1996.
31. Wolfe, L. A., Mullin, R. J., Laethem, R., Blumenkopf, T. A., Cory, M., Miller, J. F., Keith, B. R., Humphreys, J., and Smith, G. K. Antibody-directed enzyme prodrug therapy with the T268G mutant of human carboxypeptidase A1: *in vitro* and *in vivo* studies with prodrugs of methotrexate and the thymidylate synthase inhibitors GW1031 and GW1843. *Bioconjug. Chem.*, 10: 38-48, 1999.
32. Marnis, R., Spooner, R. A., Stribbling, S. M., Light, Y., Martin, J., and Springer, C. J. A cell surface tethered enzyme improves efficiency in gene-directed enzyme prodrug therapy. *Nat. Biotech.*, 15: 1373-1377, 1997.
33. Vokes, E. E. Head and neck cancer. *In: M. C. Perry (ed.), The Chemotherapy Source Book*, Ed. 2, pp. 1083-1101. Baltimore: Williams and Wilkins, 1998.
34. O'Malley, B. W., Jr., Cope, K. A., Johnson, C. S., and Schwartz, M. R. A new immunocompetent murine model for oral cancer. *Arch. Otolaryngol.*, 123: 20-24, 1997.
35. Hamstra, D. A., Rice, D. J., Fahmy, S., Ross, B. D., and Rehemtulla, A. Enzyme/prodrug therapy for head and neck cancer using a catalytically superior cytosine deaminase. *Hum. Gene Ther.*, 10: 1993-2003, 1999.

EXHIBIT B

New Advances in the Transport of Doxorubicin through the Blood-Brain Barrier by a Peptide Vector-Mediated Strategy

CHRISTOPHE ROUSSELLE, PHILIPPE CLAIR, JEANNE-MARIE LEFAUCONNIER, MICHEL KACZOREK, JEAN-MICHEL SCHERRMANN, and JAMAL TEMSAMANI

Institut National de la Santé et de la Recherche Médicale U26, Hôpital Fernand Widal, Paris, France (C.R., J.-M.L., J.-M.S.); and Syntem, Nîmes, France (P.C., M.K., J.T.)

Received June 30, 1999; accepted January 4, 2000

This paper is available online at <http://www.molpharm.org>

ABSTRACT

Many therapeutic drugs are excluded from entering the brain, due to their lack of transport through the blood-brain barrier (BBB). To overcome this problem, we have developed a novel method in which short, naturally derived peptides (16–18 amino acids) cross the cellular membranes of the BBB with high efficiency and without compromising its integrity. The antineoplastic agent doxorubicin (dox) was coupled covalently to two peptides, *D*-penetratin and SynB1. The ability of dox to cross the BBB was studied using an *in situ* rat brain perfusion technique and also by *i.v.* injection in mice. In the brain perfusion studies, we first confirmed the very low brain uptake of free radiolabeled dox because of the efflux activity of P-glycoprotein at the BBB. By contrast, we have demonstrated that when

dox is coupled to either the *D*-penetratin or SynB1 vectors, its uptake was increased by a factor of 6, suggesting that the vectorized dox bypasses P-glycoprotein. Moreover, using a capillary depletion method, we have shown that vectorization of dox led to a 20-fold increase in the amount of dox transported into brain parenchyma. Intravenous administration of vectorized dox at a dose of 2.5 mg/kg in mice led to a significant increase in brain dox concentrations during the first 30 min of postadministration, compared with free dox. Additionally, vectorization led to a significant decrease of dox concentrations in the heart. In summary, our results establish that the two peptide vectors used in this study enhance the delivery of dox across the BBB.

Drug delivery into the brain is often restricted by the blood-brain barrier (BBB), which regulates the exchange of substances between the peripheral circulation and the central nervous system. BBB acts first as an anatomical barrier because of the monolayer of endothelial cells, which are its main component. They exhibit specific properties such as the intercellular tight junctions, which prevent paracellular transport. More recently, the 170-kDa ATP-dependent efflux pump P-glycoprotein (P-gp), first described as participating in the multidrug resistance (MDR) mechanisms of tumor-cell drug resistance (Juliano and Ling, 1976) has been shown to be present at the luminal site of the endothelial cells of the BBB (Cordon-Cardo et al., 1989). As a result of the P-gp functional orientation (i.e., from brain to blood), P-gp may restrict the brain entrance or increase the brain clearance of a broad number of therapeutic compounds, including cytotoxic drugs (Gottesman and Pastan, 1993; Tsuji, 1998). As a consequence of P-gp expression at the BBB interface and overexpression at the tumoral cell level, the bioavailability of

anticancer agents, which may act within the cellular compartment to treat brain tumors, is extremely low, which explains the failure of brain tumor chemotherapy (Blasberg and Groothuis, 1986). To overcome the limited access of drugs to the brain, different methods have been developed that achieve BBB uptake. Most of these methods are invasive and are characterized by intraventricular drug infusion or disruption of the BBB (Chamberlain et al., 1993; Kroll and Neuwelt, 1998). In the case of chemotherapeutic agents, few studies have explored the structural modification of drugs to bypass MDR (Klopman et al., 1997) or coadministration of the drug with P-gp modulators that inhibit the effect of P-gp at the BBB (Colombo et al., 1994; Drion et al., 1996; Hughes et al., 1998). Carrier-based approaches have also been developed. They consist, for example, of increasing drug delivery to the brain by the use of liposomes and nanoparticles (Huwylar et al., 1996; Mayer, 1998; Schroeder et al., 1998) or attachment of the drug to peptide-vectors transported into the brain by absorptive transcytosis through the BBB (see Pardridge, 1997, and references therein).

The pegelin and penetratin peptides (18 and 16 amino acids, respectively) translocate efficiently through biological membranes and have provided the basis for the development

This study was supported partly by the Anvar Languedoc Roussillon and by the European Economic Community (contract no. BIO-CT98-0227).

This article is dedicated to Prof. Alain Bonnet, who passed away in November 1999.

ABBREVIATIONS: BBB, blood-brain barrier; P-gp, P-glycoprotein; dox, doxorubicin; MDR, multidrug resistance; TFA, trifluoroacetic acid; DMF, dimethylformamide; TDA, tissue distribution advantage.

of new peptide-conjugated drugs for transport through BBB. Pegelin (such as SynB1) peptides are derived from natural peptides called protegrins (Harwig et al., 1995; Mangoni et al., 1996). They possess an amphipathic structure in which the positively charged and hydrophobic residues are separated in the sequence. They are thought to form an antiparallel β -sheet, constrained by two disulfide bridges (Aumelas et al., 1996). Replacement of the four cysteines with serines leads to linear peptides (pegelin) that are able to cross cell membranes efficiently without any cytolytic effect. The penetratin peptides are derived from the transcription factor antennapedia (Derossi et al., 1998). The region of the homeodomain of antennapedia responsible for internalization has been mapped to its third helix (Derossi et al., 1994). This finding has led to the demonstration that a 16-amino-acid peptide corresponding to the third helix translocates efficiently across biological membranes.

The aim of this study was to assess the efficacy of these peptides as vectors for delivery of drugs through the BBB. Doxorubicin (dox) was chosen as the vectorized drug because it is a widely used antineoplastic agent in the treatment of several cancers and has been shown to poorly cross the BBB and not to penetrate the brain tumor cells because of MDR mechanisms (Ohnishi et al., 1995; Mankhetkorn et al., 1996). Various methods, such as the *in situ* brain perfusion technique (Takasato et al., 1984), have been used to evaluate brain uptake kinetics of drugs. We have applied this latter technique with some modifications (Smith, 1996). This method is simple and sensitive and allows the BBB to be exposed for a short time (15 to 90 s) to a drug under infusion conditions where the fluid composition and the rate of infusion are controlled. Complementary techniques were associated with it to measure the fraction of dox trapped into microvessel cells or present in brain parenchyma (Triguero et al., 1990). Finally, we investigated the overall bioavailability of the free and peptide-conjugated dox in mice. The results obtained in this study indicate that this approach could be used as a safe and effective delivery system for the transport of drugs across the BBB.

Materials and Methods

Animals and Reagents

Male Sprague-Dawley rats (250–350 g; 8 weeks) were obtained from Iffa-Credo (L'Arbresle, France). Mice NMRI-nude (29 g; 7 weeks) were obtained from Janvier Breeding Center (Le Genest Saint Isle, France). Animals were maintained under standard conditions with *ad libitum* access to food and water. Rats were anesthetized with an *i.p.* injection of the combination ketamine hydrochloride

(50 mg/ml; 70 mg/kg; Parke-Davis, Courbevoie, France) and diazepam (5 mg/ml; 7 mg/kg; Roche, Neuilly-Sur-Seine, France). Mice were anesthetized with isoflurane before sacrifice. The ethical rules of the French Ministry of Agriculture for experimentation with laboratory animals (law no. 87–848) were followed.

Preparation and Characterization of Peptide Conjugates

Peptide Synthesis. The peptides were assembled by conventional solid phase chemistry using a 9-fluorenylmethoxycarbonyl/tert-butyl protection scheme (Atherton and Sheppard, 1989) and purified on preparative C18 reversed phase HPLC after trifluoroacetic acid (TFA) cleavage/deprotection. The lyophilized products were assessed by C18 reversed phase analytic HPLC. The peptide sequences were SynB1 (RGGRLSYSRRRFSTSTGR; molecular mass, 2099 D) and D-penetratin (rqikiwqqrnmkwwk, the amino acids are in *D* form; molecular mass, 2245 D).

Dox-D-Penetratin Synthesis. Dox hydrochloride (1 molar equivalent; Fluka, Buchs, Switzerland) was suspended in dimethylformamide (DMF) containing diisopropylamine (2 molar equivalents; Fluka) (Fig. 1). *N*-hydroxysuccinimidylmaleimidopropionate (1 molar equivalent; Fluka) was added and incubated for 20 min. The thiol-containing peptide (either as a cysteine or as amino-terminal 3-mercaptopropionic acid solubilized in DMF) was then added to this reaction mixture, followed by a 20-min incubation. The acceptance criteria for the peptide and conjugates was HPLC purity of >98% at 215 and 480 nm in accordance with the molecular weight and fragmentation pattern for mass spectrometry. The molecular mass was found to be 3005 Da.

Dox-SynB1 Synthesis. Dox hydrochloride was suspended in DMF containing diisopropylamine (Fig. 1). Succinic anhydride (1 molar equivalent; Fluka) dissolved in DMF was added and incubated for 20 min. The resulting dox hemisuccinate was then activated by addition of benzotriazol-1-yl-oxopyrrolidinephosphonium hexafluorophosphate (1.1 molar equivalents; Novabiochem) dissolved in DMF. The peptide was then added to the reaction mixture after 5 min of activation and left for another 20 min for coupling. Further processing and purity check of the conjugate was performed as described above. The molecular mass was 2723 Da.

Radiolabeling of Dox-D-Penetratin and Dox-SynB1. Preparations were performed as described above, except that [14 C]dox (55 mCi/mmol, 2.04 TBq/mol; Amersham, Les Ulis, France) was kept limiting by raising the stoichiometry of peptide, linkers, and activators to 1.3 eq in the coupling reactions. The specific activity of both compounds was (55 mCi/mmol, 2.04 Tbq/mol) and the molar ratio of dox/peptide was 1:1. The radiochemical purity was estimated to be >98% according to the 480-nm chromatograms.

Distribution Coefficient Determinations. The lipophilicity of the radiolabeled free and vectorized dox was estimated by measuring their partitioning between the perfusion buffer, pH 7.4, and 1-octanol. Distribution coefficients ($D_{\text{octanol/buffer}}$) were determined at volume ratios of 1:1 by vigorously shaking the two phases together. The samples were then incubated at 37°C for 30 min to facilitate phase separation. One sample of each phase was weighed and the radioac-

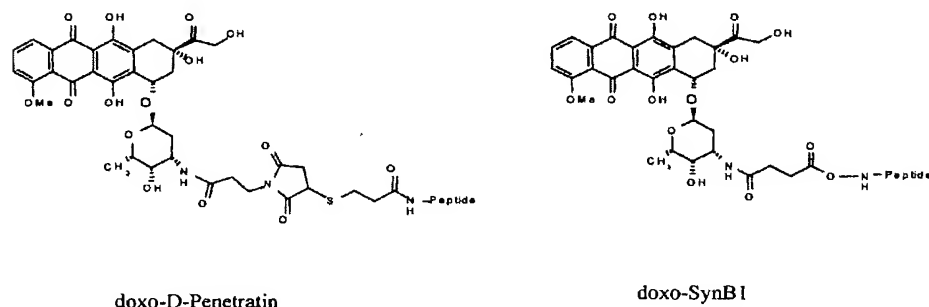


Fig. 1. Structure of dox-D-penetratin and dox-SynB1.

tivity counted in a gamma counter. $D_{\text{octanol/buffer}}$ was calculated as: (dpm/ml) in the octanol phase) / (dpm/ml) in the buffered saline phase). Experiments were done in triplicate and the mean of the log $D_{\text{octanol/buffer}}$ for dox, dox-D-penetratin, and dox-SynB1 were: 0.45 ± 0.06 ; -0.9 ± 0.08 ; and -1.44 ± 0.04 , respectively.

Plasma Protein Binding Determination. Binding to rat plasma proteins of the radiolabeled free and vectorized dox was determined after incubation of each compound in rat plasma (Iffa Credo, L'arbresle, France) for 10 min at 37°C and ultrafiltration of the samples using the Centrifree Micropartition System (Amicon, Beverly, MA). Final concentrations in both phases were determined by counting the radioactivity as described above, and the bound fraction was calculated after three experiments. For dox, dox-D-penetratin, and dox-SynB1, mean values of bound fractions were: 87.66 ± 1.76 , 99.49 ± 0.02 , and $95.8 \pm 0.38\%$, respectively.

In Situ Brain Perfusion

Blood to Brain Transfer of Dox. We used the in situ brain perfusion technique of Takasato et al. (1984) as described previously (Rouselle et al., 1998). The perfusion fluid was a bicarbonate-buffered physiological saline (128 mM NaCl, 24 mM NaHCO_3 , 4.2 mM KCl, 2.4 mM NaH_2PO_4 , 1.5 mM CaCl_2 , 0.22 mM MgSO_4 , and 9 mM D-glucose, pH 7.4) infused at a flow rate of 10 ml/min. For some experiments, rat brains were perfused with plasma obtained the same day from heparinized donor rats at a flow rate of 5 ml/min, which is sufficient to perfuse the ipsilateral hemisphere at a reasonable pressure. [^{14}C]Dox (0.3 $\mu\text{Ci/ml}$), [^{14}C]dox-D-penetratin (0.1 $\mu\text{Ci/ml}$), and [^{14}C]dox-SynB1 (0.1 $\mu\text{Ci/ml}$) were infused into the internal carotid artery for 60 s. [^3H]Sucrose (12.3 Ci/mmol; 1 $\mu\text{Ci/ml}$; NEN, Paris, France) was used for each experiment as a marker of the BBB integrity. Some rats ($n = 9$) were also pretreated 5 min before perfusion with i.v. (\pm)-verapamil hydrochloride (1 mg/kg; Sigma, St. Quentin Fallavier, France) dissolved in 0.5 ml of 0.9% NaCl.

At the end of the perfusion, the rat was decapitated and the brain quickly removed. The right cerebral hemisphere was dissected on ice in six brain areas (frontal, occipital and parietal cortex, thalamus, hippocampus, and striatum). Brain regions and 50 μl of perfusion fluid were placed in preweighed scintillation vials and weighed. Brain and perfusion fluid samples were digested for 2 h in 1 ml of Soluene-350 (Packard, Rungis, France) at 60°C. Scintillation cocktail (10 ml; Picofluor, Packard) was added to each vial and the tracer contents were assessed by dual-label liquid scintillation counting program in a Tri-Carb model 1900TR liquid scintillation counter (Packard).

Dox uptake was expressed as a single-time-point, unidirectional transfer constant (K_{in}). Briefly, calculations were accomplished as described (Smith, 1996) from the relationship $K_{\text{in}} = (Q_{\text{tot}} - V_v \cdot \text{Cpf}) / T \cdot \text{Cpf}$, where Q_{tot} is the measured quantity of [^{14}C]dox in brain (vascular and extravascular) at the end of the experiment, V_v is the cerebral vascular volume, Cpf is the perfusion fluid concentration of [^{14}C]dox, and T is the perfusion time in seconds. V_v was evaluated by the sucrose space and calculated by the ratio between radioactivity of [^3H]sucrose (expressed in dpm of sucrose per gram of brain) and the perfusate sucrose concentration.

Washing Procedure. For this set of experiments, we used a dual-syringe infusion pump (Harvard Apparatus, Les Ulis, France) with one syringe containing the bicarbonate-buffered physiological saline with the radiotracer (syringe A) and the other without radiotracer (syringe B). The carotid catheter was connected to a four-way valve (Hamilton, Bonnaduz, Switzerland). After the carotid cannulation was completed and the appropriate connections were made, syringe A was discharged at a rate of 10 ml/min for 60 s. Syringe A was switched off and syringe B was switched on simultaneously to initiate the wash-out of the capillary space. After 30 s, the rat was decapitated. The transfer constant was measured using the equation $K_{\text{in}} = Q_{\text{tot}} / T \cdot \text{Cpf}$, where Q_{tot} is the quantity of [^{14}C]dox in the extravascular brain.

Distribution in Brain Compartments. The distribution of [^{14}C]dox between brain microvascular and parenchymal compartments was assessed using the capillary depletion method of Triguero et al. (1990) with some modifications (Benrabh and Lefauconnier, 1996). Rats were perfused as described for the washing procedure. At the end of the wash-out, the right cerebral hemisphere was removed, cleaned of meninges and choroid plexus, weighed, and homogenized in 3.5 ml of capillary buffer (10 mM HEPES, 141 mM NaCl, 4 mM KCl, 1 mM NaH_2PO_4 , 2.8 mM CaCl_2 , 1 mM MgSO_4 , and 10 mM D-glucose, pH 7.4) on ice. After 15 strokes, 4 ml of a chilled 40% neutral dextran solution was added to obtain a final concentration of 20%. All homogenizations were performed at 4°C in a very short time. After taking an aliquot of homogenate, the solution was centrifuged at 5400g for 15 min at 4°C in a swinging-bucket rotor. The pellet and supernatant were carefully separated and counted in the liquid scintillation counter. The pellet was composed mainly of brain capillaries and the supernatant reflected brain parenchyma.

Dox distribution in brain compartments was expressed as distribution volume (V_d ; $\mu\text{l/g}$), defined as $V_d = Q_{\text{tis}} / \text{Cpf}$, where Q_{tis} is the measured quantity of [^{14}C]dox in brain compartments (total dpm per compartment/brain tissue weight) and Cpf is the perfusion fluid concentration (dpm/milliliters of perfusate).

Statistical Analysis. All experiments were performed on three to six rats. Data are expressed for individual cerebral areas or as the main value of the right cerebral hemisphere. Statistical comparisons conducted herein were accomplished by Student's test or ANOVA. Bonferroni's multiple comparison test was used post hoc only when ANOVA results were significant. Statistical difference was accepted at the $P < .05$ significance level. Data are presented as mean \pm S.E.

Intravenous Administration in Mice

Dox and dox-SynB1 were i.v. injected in female Nude mice (via the tail vein) at a dose of 2.5 mg/kg (mg base of dox/kg; in 200 μl of NaCl 0.9%), which corresponded to 0.5 μCi per animal. At 1, 5, 15, 30, 60, 180, 480, and 1280 min after injection, animals (five animals per group) were anesthetized before sacrifice. Mice were sacrificed by cardiac puncture and blood samples were collected in glass tubes containing EDTA anticoagulant. Brain, heart, lungs, liver, and kidneys were removed for determination of total radioactivity. The plasma was recovered after centrifugation. The tissue samples were collected in scintillation tubes, immersed in liquid nitrogen, and stored at -20°C until analysis. The samples were fully used to quantify the radioactivity, and the radioactivity data was corrected in accordance with the quenching calculation. After radioactivity measurement, the results were transformed in micrograms of dox-equivalent per gram of plasma or tissue and represented as a mean \pm S.E. of four to five animals.

Tissue to plasma partition coefficient (K_p) was determined by dividing the area under the average curve (AUC) calculated by the linear trapezoidal method for each time point between the tested tissue and plasma as $K_p \text{ } t_n \rightarrow t_{n+1} = \text{AUC } t_n \rightarrow t_{n+1} \text{ tissue} / \text{AUC } t_n \rightarrow t_{n+1} \text{ plasma}$.

The term "tissue distribution advantage" (TDA) previously used by others (Malhotra et al., 1994) was introduced to evaluate the relative uptake behavior of dox-SynB1 versus free dox. TDA was calculated as the ratio of the respective tissue to plasma partition coefficients of the conjugated dox versus free dox at each time point according to $\text{TDA} = K_p \text{ } t_n \rightarrow t_{n+1} \text{ dox-SynB1} / K_p \text{ } t_n \rightarrow t_{n+1} \text{ dox}$. A TDA > 1 will define a specific tissue targeting of SynB1.

Stability In Vitro and In Vivo

Dox-SynB1 (1 ml) solution (2 mg/ml) was mixed with 4 ml of rat or mouse plasma (obtained from Iffa-Credo). At various times (0, 15, 25, 30, 40, 45, 60, 120, 180, and 210 min), 250- μl aliquots were withdrawn and quenched in 1 ml of acid mixture ($\text{H}_2\text{O}/\text{TFA}$ 0.1%). The vectorized dox and metabolites were then extracted from plasma by applying the sample on a C18 solid phase extraction cartridge and

eluting in 500 μ l of acetonitrile/isopropanol/ H_2O /TFA (50/20/30/5 ml) solution. The samples were then analyzed by HPLC on C18 column using acetonitrile/water gradient. The percentage of nondegraded vectorized dox and released dox was calculated.

In the *in vivo* stability study, mice were *i.v.* injected with dox-SynB1 at a dose of 2.5 mg/kg (milligram base of dox). The percentage of free released dox was measured by HPLC.

Results

First, the tolerance of the BBB for the compounds used in this study was explored. [3H]sucrose was used as a marker of brain vascular volume because it does not measurably penetrate the BBB during brief periods of perfusion. When 0.05 mg of either free or coupled dox were perfused, the vascular volumes were not significantly different among brain regions in all groups. They were about 10 μ l/g of brain and of the same order of magnitude as those found in previous reports using the *in situ* brain perfusion method (Drion et al., 1996; Rousselle et al., 1998). This indicates that the permeability of the BBB was not changed. However, when 0.8 mg of dox-D-penetratin was perfused in rats, brain vascular volumes were 2-fold larger than those observed with other compounds or with 0.05 mg of dox-D-penetratin. Interestingly, the use of D-penetratin alone at the same concentration did not change the BBB permeability (data not shown), suggesting that alteration of the BBB may be caused by the complex dox-D-penetratin. We therefore used 0.05 mg of dox-D-penetratin or dox-SynB1 for the following brain perfusion experiments.

We then compared the brain uptake of free and coupled radiolabeled dox by measuring the total radioactivity in the brain after 60 s of brain perfusion. This perfusion time was chosen because it is short enough to limit the risks of drug metabolism or efflux from brain to blood but high enough to measure reasonable quantities of radiolabeled dox in brain tissues compared with the background noise of the detection method. Figure 2 shows that conjugation of dox with peptide vectors significantly enhances its brain uptake. An average

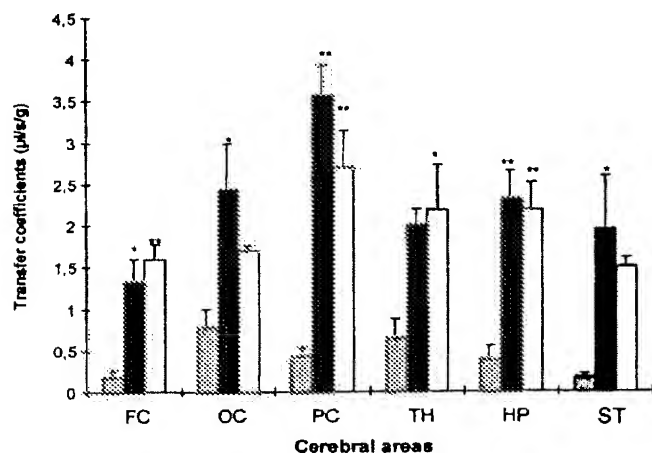


Fig. 2. Transfer coefficients (K_{in}) for [^{14}C]dox, [^{14}C]dox-D-penetratin, and [^{14}C]dox-SynB1 uptake in six areas of rat brain after perfusion with buffer. Each bar represents a mean (\pm S.E.) for $n = 4$ animals. The animals were perfused for 60 s with 5.4 nmol/ml of dox (gray columns), 1.8 nmol/ml of dox-D-penetratin (filled columns), and 1.8 nmol/ml of dox-SynB1 (open columns). FC, OC, and PC, frontal, occipital and parietal cortex; TH, thalamus; HP, hippocampus; ST, striatum. ** $P < .01$; * $P < .05$ versus free dox.

of 6-fold increase in brain uptake was obtained for both dox-D-penetratin and dox-SynB1. To assess the brain distribution of these compounds, the brain was dissected into various areas: frontal, parietal, and occipital cortex, thalamus, hippocampus, and striatum. In rats perfused with dox, the brain uptake of this compound was very low and ranged from 0.18 ± 0.04 μ l/s/g for the striatum to 0.78 ± 0.22 μ l/s/g for the occipital cortex. Vectorization with either D-penetratin or SynB1 significantly increased the brain uptake of dox after 60 s of buffer perfusion in all six gray areas. The brain uptake of dox-SynB1 ranged from 1.6 ± 0.2 μ l/s/g for the frontal cortex to 2.7 ± 0.4 μ l/s/g for the parietal cortex. In the case of dox-D-penetratin, the brain uptake ranged from 1.4 ± 0.3 μ l/s/g for the striatum to 3.6 ± 0.3 μ l/s/g for the parietal cortex.

To evaluate whether free or coupled dox has actually crossed the BBB or is simply trapped within brain endothelial cells, two experiments were performed. In the first one, the brain was perfused for 60 s with radiolabeled compounds in physiological saline followed by a 30-s washing with tracer-free saline to remove tracer bound to the capillary luminal membrane. The total radioactivity measured was then compared with the one in animals that did not receive the wash-out procedure. After the washing procedure, the cerebral uptake of free and vectorized dox was significantly reduced, indicating that this procedure removed any [^{14}C]dox trapped within the microvessels or bound to the luminal membrane of its endothelium (Fig. 3). However, in rats perfused with either dox-D-penetratin or dox-SynB1, the brain uptake was still significantly increased (2.14 ± 0.23 and 1.50 ± 0.28 μ l/s/g, respectively) compared with that of dox alone (0.25 ± 0.09 μ l/s/g). In the second experiment, distribution in the brain capillary and parenchymal compartment was measured after perfusion and wash-out using the capillary depletion method of Triguero et al. (1990), which separates the whole brain into endothelial enriched (pellet) and depleted (supernatant) fractions. This procedure distinguishes between compounds remaining in the endothelial cells from those having crossed the abluminal endothelial membrane to enter the brain parenchyma. By this method, we have observed that about 50% of the dox-derived radioactivity was associated with the capillary, whereas less than 30% of the vectorized dox-derived radioactivity was in the endothelial

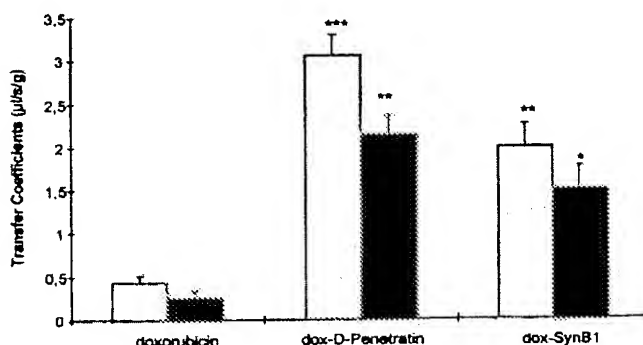


Fig. 3. Transfer coefficients (K_{in}) for [^{14}C]dox, [^{14}C]dox-D-penetratin, and [^{14}C]dox-SynB1 uptake in right hemisphere of rat brain after 60-s perfusion with buffer and 30 s of wash-out. Values are mean \pm S.E. ($n = 4$ rats). *** $P < .001$; ** $P < .01$; * $P < .05$ versus free dox. Filled columns, wash-out; gray columns, no wash-out.

cells after 60 s of perfusion followed by 30 s of wash-out (Fig. 4). In the parenchymal compartment, the ratio of vectorized dox versus free dox was about 20 for both peptide-vectors.

To compare the vectorization of dox with the effect of a P-gp inhibitor, dox uptake was evaluated in rats pretreated with (\pm)-verapamil. This calcium-channel blocker is a P-gp inhibitor commonly used to reverse MDR in cell culture (Ford and Hait, 1990). Pretreatment with verapamil only slightly increased the cerebral uptake of dox after 60 s of perfusion and 30 s of wash-out (Table 1). However, this increase was not significant. Moreover, no change in brain uptake of vectorized dox was observed after pretreatment with verapamil.

Finally, we investigated the effect of plasma protein binding on brain transfer of free and vectorized dox (Fig. 5). When the perfusion buffer was replaced by rat plasma, a dramatic decrease in dox-D-penetratin cerebral uptake was observed (0.05 versus 2.30 $\mu\text{l/s/g}$). The brain uptake of free dox was also significantly reduced (0.07 versus 0.44 $\mu\text{l/s/g}$) as it was for dox-SynB1 (0.60 versus 2.20 $\mu\text{l/s/g}$). Similar results were obtained after perfusion in the presence of 5% BSA in the saline buffer (data not shown). This is not surprising, because it has been shown previously that dox binds to plasma proteins and principally to albumin (Celio et al., 1982). Cerebral transfer coefficients of vectorized dox in plasma are also well correlated with the plasma protein binding measured in our study by ultrafiltration (87.8% for dox, 99.5% for dox-D-penetratin, and 95.8% for dox-SynB1). Consequently, we considered the possibility that the high protein binding of our peptide vectors may compromise dox delivery to the brain after peripheral administration.

To check this last hypothesis and to confirm the ability to distribute more dox in the brain, we carried out *in vivo* experiments using *i.v.* injection. Free and SynB1-conjugated radiolabeled dox were injected into mice at a dose of 2.5 mg/kg (mg base of dox) via the tail vein. After different time points, the mice were sacrificed and the total radioactivity in plasma, brain, heart, lungs, kidneys, and liver was counted. After *i.v.* injection, the tissue and plasma distribution of dox-derived radioactivity were dramatically modified when the drug was conjugated to SynB1 (Fig. 6A). The plasma concentrations were higher for dox-SynB1 and decreased less rapidly than for the free dox. The brain distribution of dox

was also apparently improved when the drug was conjugated to SynB1 (Fig. 6B). Interestingly, in the heart, where dox exerts its major toxicity, vectorization significantly reduced the dox concentrations (Fig. 6C). A similar decrease in accumulation of vectorized dox was observed in lungs. In kidneys and liver, a slight decrease in total radioactivity was observed for dox-SynB1 1 h after administration (data not shown). We also carried out a small-scale pilot experiment using D-penetratin as a vector and similar results as for SynB1 were obtained (data not shown).

To assess whether the modifications in tissue distribution observed with dox-SynB1 versus free dox were caused only by an alteration of dox-SynB1 plasma pharmacokinetics, we calculated tissue-to-plasma-partition coefficients at each time point (Table 2) and compared them with those of dox alone. The calculated TDA was found to be >1 in brain during the first 30 min after administration, showing a more important brain uptake of dox-SynB1 than would have been expected from the observed increase of dox-SynB1 plasma levels (Fig. 7). In contrast, TDAs were <1 for heart, lungs, liver, and kidneys, showing a reduction in tissue exposure for these organs at all time points.

To assess the stability and the fate of the dox-vector complex, we have carried out two preliminary experiments. In the first experiment, dox-SynB1 was incubated in rat and mouse plasma *in vitro*, and after various times, the fate and stability of the dox-SynB1 was analyzed by HPLC. Our results show that the conjugate has a degradation half-life of about 15 min in mice and rat plasma. The percentage of dox

TABLE 1

Transfer coefficients for [^{14}C]dox, [^{14}C]dox-D-penetratin, and [^{14}C]dox-SynB1 uptake into rat brain. Data are presented as mean \pm S.E.; $n = 3-6$. Perfusion time was 60 s and wash-out time was 30 s. Pretreatment with verapamil was carried out 5 min before perfusion at 1 mg/kg.

	K_{in}	
	Control	Verapamil Pretreated
	$\mu\text{l/s/g}$	
Dox	0.25 ± 0.09	0.36 ± 0.01
Dox-D-Penetratin	2.31 ± 0.46	2.15 ± 0.34
Dox-SynB1	1.20 ± 0.17	1.31 ± 0.13

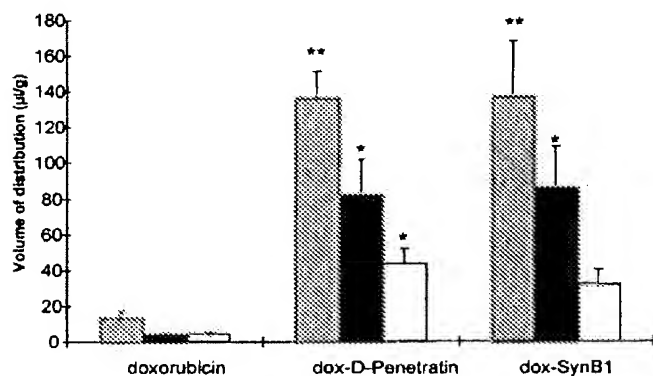


Fig. 4. Distribution volumes of [^{14}C]dox, [^{14}C]dox-D-penetratin, and [^{14}C]dox-SynB1 in vascular pellet and supernatant fractions after wash-out after the capillary depletion method. Values are mean \pm S.E. ($n = 4$ rats). ** $P < .01$; * $P < .05$ versus free dox. Gray columns, homogenate; filled columns, parenchyma; open columns, endothelial cells.

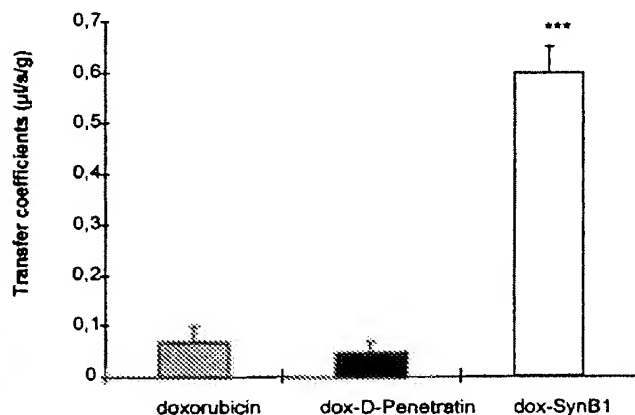


Fig. 5. Transfer coefficients (K_{in}) for [^{14}C]dox, [^{14}C]dox-D-penetratin, and [^{14}C]dox-SynB1 uptake in rat brain after perfusion with plasma. Each bar represents a mean \pm S.E. ($n = 4$ rats). Perfusion time was 60 s. *** $P < .001$ versus free dox.

released was about 8% at 15 min. The rest of products corresponded mainly to degradation in the peptide. In the second experiment, dox-SynB1 was injected into mice and the percentage of released dox was measured by HPLC. In plasma, we found that about 3% of free dox was released from dox-SynB1 after 5 min postadministration (data not shown).

Discussion

The discovery that synthetic peptides derived from natural peptides can be used successfully to deliver biologically active

substances inside live cells (Derossi et al., 1998; Schwarze et al., 1999) has provided the basis for developing new effective strategies for drug delivery into the brain. For this reason we have coupled the anticancer drug dox to two different peptides: D-penetratin and SynB1, which were expected to increase the delivery of dox to rat brain.

We first evaluated the brain uptake of free and coupled dox after 60 s of *in situ* rat brain perfusion. Under these conditions, we only observed a low uptake of dox, comparable with values reported previously by Ohnishi et al. (1995) using the same method. However, this permeability is lower than would be expected based on the lipophilicity of the compound ($\log D_{\text{octanol/buffer}} = 0.45$). This low brain permeability could be explained by the efflux activity of P-gp at the BBB. Dox is actually transported by P-gp expressed at the brain capillaries in the physiological state (Ohnishi et al., 1995; Van Asperen et al., 1999) and could also be transported by the more recently characterized MDR-associated protein mrp1 (Abe et al., 1994). To overcome MDR mechanisms, dox was given in combination with P-gp inhibitor. However, if such drug combinations are effective *in vitro*, the high concentration of P-gp inhibitors necessary to overcome drug efflux limits their clinical application. Furthermore, coadministration of anticancer drugs and P-gp modulators may alter anticancer drug pharmacokinetics, leading to an exacerbation of anticancer drug toxicity (Krishna et al., 1997).

By coupling dox to D-penetratin and SynB1, we expected to increase its uptake in the brain and circumvent the efflux activity of P-gp. It is noteworthy that the coupling makes the dox less lipophilic ($\log D_{\text{octanol/buffer}} = 0.45$ for dox, -0.9 for dox-D-penetratin, and -1.44 for dox-SynB1), which in fact should reduce the permeability through the BBB. However, a significant increase in dox-derived radioactive brain uptake was obtained for the conjugated drug compared with free dox for all six gray areas studied. This increase in brain uptake obtained for both vectors might be explained by the translocation properties of these vectors and also by the fact that vectorized dox is not recognized by the P-gp. This is confirmed by pretreatment with verapamil, which did not change the brain uptake of the coupled dox, and only a slight increase was observed for free dox. To demonstrate that vectorized dox is not trapped inside the endothelial cells but actually crosses the BBB, we carried out the wash-out procedure and the capillary depletion method. Our results indicate that the amount of vectorized dox that was delivered to the brain parenchyma was about 20-fold higher than free dox, suggesting the efficiency of these peptide-vectors in delivering dox to the brain parenchyma. However, we observed a decrease in brain uptake (especially for dox-D-penetratin) when the cerebral perfusion was performed with plasma for a short period of time (60 s). Over a longer period of time, protein binding does not seem to hamper the brain distribution of vectorized dox as shown by the results obtained after *i.v.* administration in mice. These results are consistent with the hypothesis that the bound drug in plasma can dissociate from proteins and thus becomes available for brain transfer. When the permeability of the brain capillaries for the free drug is sufficiently high, a new equilibrium is rapidly achieved inside the capillaries leading to the release of some bound drug into a free form that then becomes available for brain transfer (Pardridge and Landaw, 1984; Joliet-Riant and Tillement, 1999).

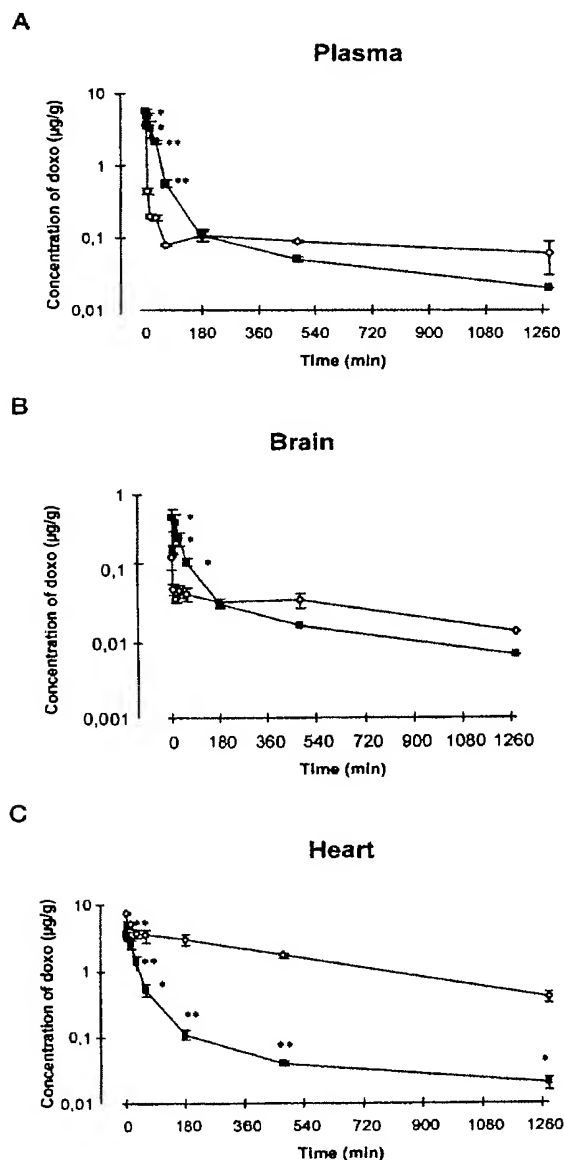


Fig. 6. Plasma and tissues distribution after *i.v.* administration of free dox (○) and dox-SynB1 (■) at a dose of 2.5 mg/kg. The concentrations are represented in microgram equivalents of dox on the basis of radioactivity measurements. The bars represent the S.E. of four to five animals. A, plasma; B, brain; C, heart. * $P < .05$; ** $P < .01$ versus free dox.

TABLE 2

The area under plasma and tissues concentration curve (AUC) values were calculated for both dox-SynB1 and free dox from the time of injection to the given time point. The ratio of AUC tissue/AUC plasma of free and vectorized dox is represented here.

Time (min)	AUC Tissue/AUC Plasma									
	Brain		Heart		Lungs		Liver		Kidneys	
	dox	dox-SynB1	dox	dox-SynB1	dox	dox-SynB1	dox	dox-SynB1	dox	dox-SynB1
1	0.017	0.044	0.9	0.325	1.165	0.307	0.311	0.324	4.414	1.511
5	0.037	0.06	2.286	0.578	3.039	0.594	0.974	0.586	7.675	3.291
15	0.059	0.069	5.041	0.65	6.503	0.809	3.109	0.746	17.341	4.183
30	0.086	0.09	7.787	0.674	9.33	1.002	5.981	0.934	25.264	4.585
60	0.136	0.104	11.072	0.677	12.604	1.174	8.967	1.222	34.52	4.959
180	0.233	0.132	18.723	0.734	22.365	1.463	12.34	1.875	50.365	5.45
480	0.295	0.153	20.959	0.767	29.263	1.793	13.164	2.492	53.588	5.924
1280	0.32	0.175	17.63	0.768	30.683	2.868	12.085	3.269	48.984	6.136

The pharmacokinetic profile of vectorized dox in plasma and tissues showed marked differences compared with free dox. In plasma, vectorization led to higher initial concentrations of dox-SynB1 than for free dox and the blood clearance of the vectorized dox was reduced during the first 180 min (area under the curve of dox-SynB1 was 5.51 times higher than for dox), allowing the compound to be more exposed to brain and other tissues. Assuming that dox-SynB1 is hydrolyzed in plasma with a stability half-life in plasma of about 15 min, this suggests that during at least 2 to 3 half-lives (i.e., 30 to 45 min) corresponding to the time window of the distribution phase, a higher tissue exposure was obtained for dox-synB1 than for free dox.

Surprisingly, we found different distribution patterns of vectorized dox in tissues compared with free dox, suggesting a tissue-specific uptake of dox-SynB1. In fact, certain tissues like heart, lungs, and, to a lower extent, kidneys and liver, had a lower uptake of dox-SynB1 than free dox (TDA were in general <0.4). The lower accumulation in heart could be of great clinical interest, because the use of dox in chemotherapy has been hampered by its cardiotoxicity (Lefrak et al., 1973). The lower uptake observed for vectorized dox in lungs can also be regarded as an interesting property, because the lung is usually the first exposed organ after the i.v. route and is known to markedly distribute cationic molecules, causing toxicity (Bummer et al., 1995). Brain, rather than these tissues, seemed to accumulate vectorized dox. During the first 180 min after administration, the brain levels of dox-SynB1 were higher than those of free dox. Nevertheless, this might result from the increase in the systemic bioavailability of dox-SynB1. To verify this hypothesis, we calculated the brain distribution advantage, which shows that during the first 30 min after administration, brain uptake enhancement was

higher than that observed in plasma. This observation confirms that during the period in which dox-SynB1 is not too much hydrolyzed, the more pronounced brain uptake results from the dox-SynB1 chemical entity interaction with endothelial cells of the BBB. This effect observed in vivo is well supported by the data from the in situ brain perfusion method, which showed a rapid transcytosis process across the BBB. For longer time-points, degraded forms of dox-SynB1 being predominant, no enhancement in dox brain uptake was observed. This suggests that enhancing the stability of the vectors might enhance the brain uptake of dox. A time balance between the kinetics of vector degradation and drug release in the targeted tissue has to be found by using less degradable amino acid sequences and appropriate linker. The challenge now is to develop peptide-vectors stable enough in plasma and a linker that will allow the drug to be cleaved off once it has crossed the BBB.

In summary, the tissue distribution shows two different organ patterns: tissues with less exposure (heart, lungs, liver, and kidneys) and tissues with higher exposure (brain). This clearly shows a tissue-specific uptake of the vectorized dox.

The mechanism by which these peptides cross the BBB is still under investigation. These peptides translocate efficiently across cell membranes and, at least in the case of D-penetratin, cell internalization does not seem to involve classical receptor-mediated endocytosis (Derossi et al., 1996). It is possible that once internalized, the peptides are addressed to a secretory compartment and re-exported into the brain parenchyma. Interestingly, Prochiantz and colleagues have demonstrated that homeoproteins—from which penetratin sequences were derived—can be secreted from live cells and gain access in vivo to a secretory compartment enriched in cholesterol and glycosphingolipids (Joliet et al., 1997, 1998).

These studies only test the feasibility of enhancing dox delivery to brain using peptide-vectors and do not address the pharmacodynamics of drug action in brain. It is crucial that the coupling of dox does not result in a loss of biological activity. Our preliminary experiments in cell culture using resistant cell lines show that the coupled dox with both D-penetratin and SynB1 bypasses P-gp and increases drug potency compared with free dox (unpublished observations). The next step will be to explore the antitumor potential of vectorized dox in brain tumor models and new modified peptides.

In conclusion, this study demonstrates the successful ap-

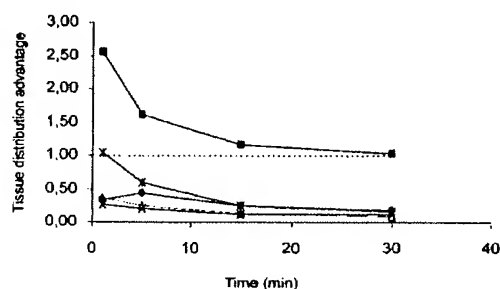


Fig. 7. TDA was calculated as the ratio of the respective tissue to plasma partition coefficients of the vectorized dox versus free dox at each time point. —, plasma; ■, brain; △, heart; ×, lungs; *, liver; ●, kidneys.

plication of the use of these peptide vectors for brain delivery of dox. A significant enhancement of dox uptake in brain was obtained after coupling dox with these peptides. Although these investigations focus on the delivery of dox, this approach should be applicable to other therapeutic drugs.

Acknowledgments

We thank Dr. Alain Prochiantz and Professor Anthony Rees for helpful advice and criticism, and Dr. Pierre Vidal for the in vitro stability work.

References

- Abe T, Hasegawa S, Taniguchi K, Yokomizo A, Kuwano T, Ono M, Mori T, Hori S, Kohno K and Kuwano M (1994) Possible involvement of multidrug-resistance-associated protein (MRP) gene expression in spontaneous drug resistance to vincristine, etoposide and adriamycin in human glioma cells. *Int J Cancer* 58:860–864.
- Atherton E and Sheppard RC (1989) *Solid Phase Peptide Synthesis: A Practical Approach*. IRL Press at Oxford University Press, Oxford, England.
- Aumelas A, Mangoni M, Roumestand C, Chiche L, Despau E, Grassy G, Calas B and Chavanieu A (1996) Synthesis and solution structure of the antimicrobial peptide protegrin-1. *Eur J Biochem* 237:575–583.
- Benrabh H and Lefauconnier JM (1996) Blood-endothelial cell and blood-brain transport of L-proline, alpha-aminobutyric acid, and L-alanine. *Neurochem Res* 21:1227–1235.
- Blasberg RG and Groothuis DR (1986) Chemotherapy of brain tumors: Physiological and pharmacokinetic considerations. *Semin Oncol* 13:70–82.
- Bummer PM, Aziz S and Gillespie MN (1995) Inhibition of pulmonary surfactant biophysical activity by cationic polyamino acids. *Pharm Res* 12:1658–1663.
- Celio LA, Digregorio GJ, Ruch E, Pace JN and Pirasino AJ (1982) Doxorubicin concentrations in rat plasma, parotid saliva, and bile and protein binding in rat plasma. *Arch Int Pharmacodyn Ther* 260:180–188.
- Chamberlain MC, Khatibi S, Kim JC, Howell SB, Chatelut E and Kim S (1993) Treatment of leptomeningeal metastasis with intraventricular administration of depot cytarabine (DTC 101). A phase I study. *Arch Neurol* 50:261–264.
- Colombo T, Zucchetti M and D'Incalci M (1994) Cyclosporin A markedly changes the distribution of doxorubicin in mice and rats. *J Pharmacol Exp Ther* 269:22–27.
- Cordon-Cardo C, O'Brien JP, Casals D, Rittman-Grauer L, Biedler JL, Melamed MR and Bertino JR (1989) Multidrug-resistance gene (P-glycoprotein) is expressed by endothelial cells at blood-brain barrier sites. *Proc Natl Acad Sci USA* 86:696–698.
- Derosi D, Calvet S, Trembleau A, Brunissen A, Chassaing G and Prochiantz A (1996) Cell internalization of the third helix of the Antennapedia homeodomain is receptor-independent. *J Biol Chem* 271:18188–18193.
- Derosi D, Chassaing G and Prochiantz A (1998) Trojan peptides: The penetrating system for intracellular delivery. *Trends Cell Biol* 8:84–87.
- Derosi D, Joliet AH, Chassaing G and Prochiantz A (1994) The third helix of the Antennapedia homeodomain translocates through biological membranes. *J Biol Chem* 269:10444–10450.
- Drion N, Lemaire M, Lefauconnier JM and Scherrmann JM (1996) Role of P-glycoprotein in the blood-brain transport of colchicine and vinblastine. *J Neurochem* 67:1688–1693.
- Ford JM and Hait WN (1990) Pharmacology of drugs that alter multidrug resistance in cancer. *Pharmacol Rev* 42:155–199.
- Gottesman MM and Pastan I (1993) Biochemistry of multidrug resistance mediated by the multidrug transporter. *Annu Rev Biochem* 62:385–427.
- Harwig SS, Swiderek KM, Lee TD and Lehrer RI (1995) Determination of disulphide bridges in PG-2, an antimicrobial peptide from porcine leukocytes. *J Peptide Sci* 1:207–215.
- Hughes CS, Vaden SL, Manaugh CA, Price GS and Hudson LC (1998) Modulation of doxorubicin concentration by cyclosporin A in brain and testicular barrier tissues expressing P-glycoprotein in rats. *J Neurooncol* 37:45–54.
- Huwyler J, Wu D and Pardridge WM (1996) Brain drug delivery of small molecules using immunoliposomes. *Proc Natl Acad Sci USA* 93:14164–14169.
- Joliet A, Maizel A, Rosenberg D, Trembleau A, Dupas S, Volovitch M and Prochiantz A (1998) Identification of a signal sequence necessary for the unconventional secretion of Engrailed homeoprotein. *Curr Biol* 8:856–863.
- Joliet A, Trembleau A, Raposo G, Calvet S, Volovitch M and Prochiantz A (1997) Association of Engrailed homeoproteins with vesicles presenting caveolae-like properties. *Development* 124:1865–1875.
- Joliet-Riant P and Tillement JP (1999) Drug transfer across the blood-brain barrier and improvement of brain delivery. *Fundam Clin Pharmacol* 13:16–26.
- Juliano RL and Ling V (1976) A surface glycoprotein modulating drug permeability in Chinese hamster ovary cell mutants. *Biochim Biophys Acta* 455:152–162.
- Klopman G, Shi LM and Ramu A (1997) Quantitative structure-activity relationship of multidrug resistance reversal agents. *Mol Pharmacol* 52:323–334.
- Krishna R, De Jong G and Mayer LD (1997) Pulse exposure of SDZ PSC 833 to multidrug resistant P388/ADR and MCF7/ADR cells in the absence of anticancer drugs can fully restore sensitivity to doxorubicin. *Anticancer Res* 17:3329–3334.
- Kroll RA and Newell EA (1998) Outwitting the blood-brain barrier for therapeutic purposes: Osmotic opening and other means. *Neurosurgery* 42:1083–1099.
- Lefrak EA, Pitha J, Rosenheim S and Gottlieb JA (1973) A clinicopathologic analysis of adriamycin cardiotoxicity. *Cancer* 32:302–314.
- Malhotra BK, Lemaire M and Sawchuk J (1994) Investigation of the distribution of cab 515 to cortical ECF and CSF in freely moving rats utilizing microdialysis. *Pharmacol Res* 11:1223–1232.
- Mangoni ME, Aumelas A, Charnet P, Roumestand C, Chiche L, Despau E, Grassy G, Calas B and Chavanieu A (1996) Change in membrane permeability induced by protegrin 1: Implication of disulphide bridges for pore formation. *FEBS Lett* 383:93–98.
- Mankhetkorn S, Dubru F, Hesschenbrouck J, Fiallo M and Garnier-Suillerot A (1996) Relation among the resistance factor, kinetics of uptake, and kinetics of the P-glycoprotein-mediated efflux of doxorubicin, daunorubicin, 8-(S)-fluoridaurubicin, and idarubicin in multidrug-resistant K562 cells. *Mol Pharmacol* 49:532–539.
- Mayer LD (1998) Future developments in the selectivity of anticancer agents: Drug delivery and molecular target strategies. *Cancer Metastasis Rev* 17:211–218.
- Ohnishi T, Tamai I, Sakanaka K, Sakata A, Yamashita T, Yamashita J and Tsuji A (1995) In vivo and in vitro evidence for ATP-dependency of P-glycoprotein-mediated efflux of doxorubicin at the blood-brain barrier. *Biochem Pharmacol* 49:1541–1544.
- Pardridge WM (1997) Drug delivery to the brain. *J Cereb Blood Flow Metab* 17:713–731.
- Pardridge WM and Landaw EM (1984) Tracer kinetic model of blood-brain barrier transport of plasma protein-bound ligands. Empiric testing of the free hormone hypothesis. *J Clin Invest* 74:745–752.
- Rousselle CH, Lefauconnier JM and Allen DD (1998) Evaluation of anesthetic effects on parameters for the in situ rat brain perfusion technique. *Neurosci Lett* 257:139–142.
- Schroeder U, Sommerfeld P, Ulrich S and Sabel BA (1998) Nanoparticle technology for delivery of drugs across the blood-brain barrier. *J Pharmacol Sci* 87:1306–1307.
- Schwarze SR, Ho A, Vocero-Akbani A and Dowdy SF (1999) In vivo protein transduction: Delivery of a biologically active protein into mouse. *Science (Wash DC)* 286:1569–1572.
- Smith QR (1996) Brain perfusion systems for studies of drug uptake and metabolism in the central nervous system. *Pharm Biotechnol* 8:285–307.
- Takasato Y, Rapoport SI and Smith QR (1984) An in situ brain perfusion technique to study cerebrovascular transport in the rat. *Am J Physiol* 247:H484–H493.
- Triguero D, Buciak J and Pardridge WM (1990) Capillary depletion method for quantification of blood-brain barrier transport of circulating peptides and plasma proteins. *J Neurochem* 54:1882–1888.
- Tsuji A (1998) P-glycoprotein-mediated efflux transport of anticancer drugs at the blood-brain barrier. *Ther Drug Monit* 20:588–590.
- Van Asperen J, Van Tellingen O, Tijssen F, Schinkel AH and Beijnen JH (1999) Increased accumulation of doxorubicin and doxorubicinol in cardiac tissue of mice lacking mdr1a P-glycoprotein. *Br J Cancer* 79:108–113.

Send reprint requests to: Dr. Jamal Tamsamani, Syntem, Parc Scientifique Georges Besse, 30000 Nîmes, France. E-mail: jtamsamani@syntem.eerie.fr